Asymptotic homogenization approach for anisotropic micropolar modeling of periodic Cauchy materials

Asymptotic homogenization approach for micropolar modelling of periodic Cauchy materials

Andrea Bacigalupo[a], Maria Laura De Bellis[b], Giorgio Zavarise[c]

[a]*University of Genoa, Department DICCA, via Montallegro 1, Genoa, Italy*
[b]*University of Chieti-Pescara, Department INGEO, Viale Pindaro 42, Pescara, Italy*
[c]*Turin Polytechnic, Department DISEG, Corso Duca degli Abruzzi 24, Turin, Italy*

Abstract

A micropolar-based asymptotic homogenization approach for the analysis of composite materials with periodic microstructure is proposed. The upscaling relations, conceived to determine the macro-descriptors (macro displacement and the micropolar rotation fields) as a function of the micro displacement field, are consistently derived in the asymptotic framework. In particular, the micropolar rotation field is expressed in terms of the microscopical infinitesimal rotation tensor and the perturbation functions. The micro displacement field is, in turn, obtained by choosing a third order approximation of the asymptotic expansion, in which the macroscopic fields are expressed as a third order polynomial expansion. It follows that the macro descriptors are directly related to both perturbation functions and micropolar two-dimensional deformation modes. A properly conceived energy equivalence between the macroscopic point and a microscopic representative portion of the periodic composite material is introduced to derive the consistent overall micropolar constitutive tensors. It is pointed out that these constitutive tensors are not affected by the choice of the periodic cell. Moreover, in the case of vanishing microstructure the nonlocal constitutive tensors tend to zero, as expected. Finally, the capabilities of the proposed approach are shown through some illustrative examples.

Keywords: Periodic Cauchy materials, Micropolar continuum, Asymptotic homogenization, Microscopic mean strain energy, Overall constitutive tensors

1. Introduction

Periodic manufactured composites are widely used in many engineering fields, ranging from mechanics, through aerospace and robotics to bio-mechanics. In this context, it is crucial to accurately reproduce the material response, possibly resorting to micromechanical approaches that may require very high computational costs. At the same time, it is also fundamental to use models able to grasp the overall response, with its peculiar characteristics, in a synthetic and accurate way. In this framework, the study of multi-scale homogenization techniques, able to properly reproduce the overall behavior of periodic heterogeneous materials by exploiting the detailed information available at the microscopic scale, is a very intriguing and debated topic in literature.

The classical homogenization approaches, based on linking Cauchy continua at the microscopic and macroscopic scales, could be ineffective in the case the microstructural characteristic size is not negligible with respect either to the structural size, or to the wavelengths of both periodic forces and acoustic wave propagating in the medium, as well as in the presence of high strain and stress gradients. In such cases, the use at the macroscopic scale of non-local continua [1–3], involving characteristic lengths in the constitutive equations, enables one to reproduce more accurately the macroscopic behavior, driven by the actual heterogeneous material at the microscopic scale. In particular, the presence of these characteristic lengths allows a consistent description of dispersive waves, and an objective numerical response in the case of strain softening behavior.

The homogenization techniques proposed so far to investigate periodic Cauchy composites can be classified in three groups, that is: i) asymptotic approaches [4–13]; ii) variational-asymptotic approaches [14–17]; iii) a wide range of identification techniques, among which analytical [18–24] and computational approaches [25–49].

By exploiting the sound mathematical basis of both asymptotic and variational-asymptotic techniques, it is possible to find rigorous analytical solutions for the higher-order homogenization of periodic linear elastic heterogeneous materials. The key idea is to perform a properly conceived asymptotic expansion of the micro-displacement field in order to define a series of recursive differential problems over the periodic unit cell, in terms of microscopic variables. Downscaling relations, coupling the kinematics at both macroscopic and microscopic scales, are, then, derived consistently with solvability conditions of these non-homogeneous recursive problems. In particular, the downscaling relations are expressed in terms of macroscopic descriptors – displacement and its gradients – and so-called perturbation functions, directly depending on heterogeneities. Such perturbation functions, obtained as solution of differential cell problems in the presence of locally periodic body forces, are found to be locally periodic. This circumstance guarantees the objectivity of the results, irrespective of the choice of the periodic cell.

On the other hand, computational approaches, derived for second-order, as well as for micropolar and micromorphic continua, are heuristically based on polynomial expansions of the macroscopic kinematic fields, and have attracted the attention of the scientific community especially because of their appealing formulation and reasonable computational effort. In this context, the microscopic displacement field is assumed as the superposition of two fields. The former field is the aforementioned polynomial expansion, while the latter is an a-priori unknown micro-displacement fluctuation field. Such fluctuation field is obtained by solving differential cell problems in the absence of body forces in most cases undergoing periodic boundary conditions.

The case of micropolar homogenization, linking a micropolar continuum at the macroscopic scale with a heterogeneous Cauchy continuum at the microscopic scale, requires particular attention. It stands to reason, indeed, that the lack of a one to one correspondence between displacement degrees of freedom at both scales makes it difficult to define consistent down- and upscaling relations resorting both to standard asymptotic or computational homogenization approaches. In [25] a micropolar computational approach is proposed. The main idea is the definition of an heuristic relation between the microscopic fields and the micropolar rotation field. Also in this case, periodic boundary conditions are imposed. A principal drawback of utilizing periodic boundary conditions, with generalized continua at the macroscopic scale, is the inability of guaranteeing the C1-continuity of the micro-displacement field between adjacent cells for

some second-order or micropolar/micromorphic strain components, such as bending modes, see [32, 34]. For this reason, generalised periodic boundary conditions have been proposed in the framework of the second-order homogenization in [32], as well as in the case of micropolar homogenization in [42, 50]. Specifically, in [32, 34] a critical analysis on advantages and disadvantages of computational homogenization approaches for different generalized continua has been presented. Open issues remain on the dependence of both the fluctuation fields and homogenized constitutive parameters on the choice of the periodic cell. A further sticking point concerns the fact that in the case of vanishing microstructure, i.e. when the material tends to be homogeneous, these models are not able to recover the Cauchy medium, but in general non-zero characteristic lengths or non-local constitutive components are unexpectedly found.
In the framework of second-order homogenization, in [11] a strategy has been proposed to unambiguously determine this microscopic displacement fluctuation field via asymptotic techniques. More specifically, an analytical correlation between the overall elastic constitutive tensors obtained through asymptotic and computational approaches has been proposed, through the definition of a generalized macro-homogeneity condition between the microscopic average strain energy and the macroscopic strain energy. It is also shown that these elastic constitutive tensors are independent on the choice of the periodic cell and the Cauchy medium is recovered when the microstructure vanishes.
On the other hand, in the case of micropolar homogenization of periodic Cauchy materials these problems seem to be still unsolved, at least for the authors knowledge. Therefore, this paper focuses on a micropolar modelling of composite materials with periodic microstructure (e.g. made up by inclusions regularly embedded into a matrix) based on an asymptotic homogenization scheme. The proposed homogenization procedure is conceived for providing an objective macroscopic constitutive response, independent on the choice of the periodic cell, as well for avoiding the well-known pathological behavior found in the case of non vanishing characteristic lengths (i.e. non local elastic constants) even when the material tends to become homogeneous. The upscaling relations are inspired by those originally proposed by [25] in the framework of the computational homogenization. Such upscaling relations, consistently derived in the asymptotic framework, directly relate the macro-descriptors (macro displacements and micropolar rotation fields) to the micro displacement field. Concerning the micropolar rotation field, it is derived as a function of both the microscopical rotation tensor and the perturbation functions at different orders. In particular, the microscopic displacement field is described as superposition of the macroscopic driven third order polynomial kinematic map and the locally periodic perturbation fields. Specifically, these perturbation functions are inherently related to the heterogeneous nature of the composite medium and are derived from the solution of recursive differential cell problems. Moreover, the overall micropolar elastic tensors derive from a properly conceived energy equivalence between the macroscopic point and a representative portion of the heterogeneous material at the microscopic scale. Different applications to bi-phase orthotropic materials are performed in order to exploit the capabilities of the proposed approach.
The paper is organized as follows. In Section 2 the governing equations at both microscopic and macroscopic scales are briefly recalled. In Section 3 a synopsis of the proposed method is presented. More in detail, Section 3.1 is devoted to define the micro-macro kinematic relations and the asymptotic expansion of the microscopic governing equations. The upscaling relations and a properly defined kinematic map are, then, fully developed in Section 3.2. The generalized macro-homogeneity condition is, then, derived in Section 3.3. Some illustrative applications of technological interest are proposed in Section 4. Finally, in Section 5 some concluding remarks are reported.

2. Cauchy-micropolar homogenization

The aim of this work is to characterize a homogenized micropolar continuum at the macroscopic level, derived from the mechanical properties of the periodic heterogeneous material described as a Cauchy continuum at the microscopic scale. In the following the governing equations together with the boundary conditions at both microscopic and macroscopic scales are reported.

2.1. Microscopic governing equations of the Cauchy periodic material

In the framework of linearized kinematics, we focus on a heterogeneous composite material with periodic microstructure made up, for instance, by a regular distribution of inclusions embedded into a base matrix. A classical Cauchy continuum, subject to stresses induced by periodic body forces, is then considered. Without loss of generality and for simplicity of notation, we restrict attention to the two-dimensional case. A generic point $\mathbf{x} = x_1\mathbf{e}_1 + x_2\mathbf{e}_2$ is, thus, referred to a system of coordinates with origin at point O and orthogonal base $(\mathbf{e}_1,\mathbf{e}_2)$, as in Figure 1(a). In the periodic medium it is possible to

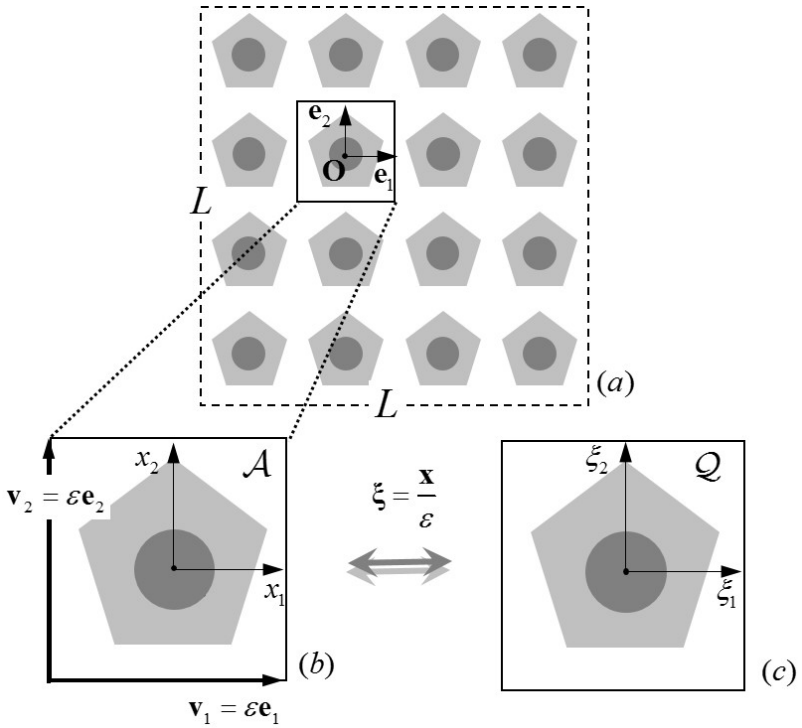

Figure 1: Heterogeneous material at the microscopic level. (a) Cluster of periodic cells with structural dimensions L; (b) Periodic Cell $\mathcal{A}$ with characteristic size ε; (c) unit cell $\mathcal{Q}$.

identify a periodic cell $\mathcal{A} = [-\varepsilon/2, \varepsilon/2] \times [-\varepsilon/2, \varepsilon/2]$, whose characteristic size is ε, having two orthogonal periodicity vectors $\mathbf{v}_1{=}d_1\mathbf{e}_1{=}\varepsilon\,\mathbf{e}_1$, and $\mathbf{v}_2{=}d_2\mathbf{e}_2{=}\varepsilon\,\mathbf{e}_2$. Therefore, the microscopic elasticity tensor $\mathbb{C}^{(m,\varepsilon)}(\mathbf{x}){=}C^{(m,\varepsilon)}_{ijhk}\mathbf{e}_i \otimes \mathbf{e}_j \otimes \mathbf{e}_h \otimes \mathbf{e}_k$ (where the superscript m stands for the microscale) is $\mathcal{A}$-periodic and fulfills the property $\mathbb{C}^{(m,\varepsilon)}(\mathbf{x} + \mathbf{v}_i) = \mathbb{C}^{(m,\varepsilon)}(\mathbf{x})$, $i{=}$ 1,2 and $\forall\mathbf{x} \in \mathcal{A}$, see Figure 1(b). Consistently with standard asymptotic homogenization approaches, the unit cell $\mathcal{Q} = [-1/2,\ 1/2] \times[-1/2, 1/2]$ is obtained by applying a rescaling factor of ε to the periodic cell $\mathcal{A}$, as shown in Figure1(c). Besides the macroscopic variable $\mathbf{x} \in \mathcal{A}$, also referred to as *slow* variable, it is, thus, possible to define the microscopic or *fast* variable $\xi{=}\mathbf{x}/\varepsilon \in \mathcal{Q}$. Accordingly, the constitutive tensor can be expressed as $\mathbb{C}^{(m,\varepsilon)}(\mathbf{x}){=}\mathbb{C}^{m}(\boldsymbol{\xi}{=}\mathbf{x}/\varepsilon)$, where the $\mathcal{Q}$-periodicity is made explicit.

In this framework, being $\mathbf{u}(\mathbf{x})$ the displacement field of each material point, the micro strain tensor $\boldsymbol{\varepsilon}(\mathbf{x}) = sym\nabla\mathbf{u}$, and the micro infinitesimal rotation tensor $\boldsymbol{\omega}(\mathbf{x}) = skw\nabla\mathbf{u}$ are defined. The classical Cauchy constitutive relations, linking the microscopic stress and strain tensors, result therefore as $\boldsymbol{\sigma}(\mathbf{x}) = \mathbb{C}^{m}(\mathbf{x}/\varepsilon)\,\boldsymbol{\varepsilon}(\mathbf{x})$, where $\boldsymbol{\sigma}(\mathbf{x})$ is the micro stress tensor. The linear momentum balance is $\nabla\cdot\boldsymbol{\sigma}(\mathbf{x}) + \mathbf{b}(\mathbf{x}) = \mathbf{0}$, where the body forces $\mathbf{b}(\mathbf{x}) = b_i\mathbf{e}_i$, i=1,2, only depend on the *slow* variable $\mathbf{x}$. It is, indeed, assumed that the body forces fulfill the $\mathcal{L}$-periodicity with $\mathcal{L} = [-L/2; L/2] \times [-L/2; L/2]$, and have zero mean values on $\mathcal{L}$. Moreover, L can be considered as a representative portion of the whole body, see Figure 1(a), under the assumption that the structural length L is much greater than the microstructural length ε ($L >> \varepsilon$), consistently with the scale separation principle.

By plugging the constitutive equations and the compatibility equations ($\boldsymbol{\varepsilon}(\mathbf{x}) = sym\nabla\mathbf{u}$) into the linear

momentum balance, and exploiting the symmetry properties of the elastic tensor, the governing equation takes the following form

$$\nabla \cdot \left(\mathbb{C}^m \left(\frac{\mathbf{x}}{\varepsilon} \right) \nabla \mathbf{u}(\mathbf{x}) \right) + \mathbf{b}(\mathbf{x}) = \mathbf{0}. \tag{1}$$

The interface conditions, applying in the periodic cell $\mathcal{A}$, expressing the continuity of displacements and tractions, are

$$[[\mathbf{u}(\mathbf{x})]]|_{\mathbf{x}\in\Gamma} = \mathbf{0}, \ [[\mathbb{C}^m \left(\frac{\mathbf{x}}{\varepsilon} \right) \nabla \mathbf{u}(\mathbf{x}) \cdot \mathbf{n}]]|_{\mathbf{x}\in\Gamma} = \mathbf{0}, \tag{2}$$

where $[[g]] = g_i(\Gamma) - g_j(\Gamma)$ is defined as the jump discontinuity of the generic function g at the interface Γ between phases i and j in $\mathcal{A}$, and $\mathbf{n}$ denotes the outward normal to the interface. The microscopic displacement field, solution of the governing equation (1) and the interface conditions (2), explicitly depends on both $\mathbf{x}$ and $\boldsymbol{\xi}$ as a result of the $\mathcal{Q}$-periodicity of the microscopic elastic tensors and the $\mathcal{L}$-periodicity of the body forces, thus giving rise to

$$\mathbf{u} = \mathbf{u}\left(\mathbf{x}, \xi = \frac{\mathbf{x}}{\varepsilon} \right). \tag{3}$$

Due to this double $\mathcal{Q}$- and $\mathcal{L}$-periodicity, the problem of finding the solution of the governing equation (1) turns out to be, in general, both very cumbersome, using numerical approaches, and very difficult or almost impractical using analytic approaches.
A possible way out is the use of homogenization techniques that allow to replace the periodic medium with an equivalent homogeneous one, resulting in governing equations characterized by constant coefficients. We here derive an equivalent micropolar continuum, which overall constitutive tensors are analytically obtained in terms of the actual geometric and mechanical properties of the microstructure.

2.2. Macroscopic governing equations of the micropolar homogenized material

At the macroscopic level, a generic material point is characterized by a generalized displacement depending on the continuum fields $\mathbf{U}(\mathbf{x})$ and $\Phi(\mathbf{x})$, playing the role of macro-displacements and micropolar rotation field, respectively, both only depending on the macroscopic (*slow*) variable $\mathbf{x}$.
The asymmetric micropolar strain tensor is $\boldsymbol{\Gamma}(\mathbf{x}) = \mathbf{H}(\mathbf{x}) - \mathbf{W}(\Phi(\mathbf{x}))$, depending on the macroscopic displacement gradient $\mathbf{H}(\mathbf{x}) = \nabla\mathbf{U}(\mathbf{x})$ and the skew-symmetric micropolar rotation tensor $\mathbf{W}(\mathbf{x}) = W_{ij}\mathbf{e}_i \otimes \mathbf{e}_j$. This latter tensor is associated to the micropolar rotation vector $\Phi\mathbf{e}_3$ (being $\mathbf{e}_3$ the unit vector orthogonal to $\mathbf{e}_1, \mathbf{e}_2$) through the relation $W_{ij} = -\varepsilon_{3ij}\Phi$, where ε_{3ij} is the Levi-Civita symbol, fulfilling the property $W_{ij}a_j = \varepsilon_{i3k}\Phi a_k$ for the generic vector $\mathbf{a} = a_k\mathbf{e}_k$. It is worth-noting that by exploiting the additive decomposition of the macroscopic displacement gradient, i.e. $\mathbf{H}(\mathbf{x}) = \mathbf{E}(\mathbf{x}) + \boldsymbol{\Omega}(\mathbf{x})$, the symmetric $\mathbf{E}(\mathbf{x}) = sym(\mathbf{H}(\mathbf{x}))$ and the skew-symmetric $\boldsymbol{\Omega}(\mathbf{x}) = sym(\mathbf{H}(\mathbf{x}))$ parts are consistently derived. Besides, the curvature tensor is introduced as $\mathbf{K}(\mathbf{x}) = \nabla\Phi(\mathbf{x})$. Therefore, the micropolar constitutive relations result as

$$\begin{aligned} \boldsymbol{\Sigma}(\mathbf{x}) &= \mathbb{G}^M \boldsymbol{\Gamma}(\mathbf{x}) + \mathbf{Y}^M \mathbf{K}(\mathbf{x}), \\ \mathbf{M}(\mathbf{x}) &= \mathbf{Y}^{M^T} \boldsymbol{\Gamma}(\mathbf{x}) + \mathbf{S}^M \mathbf{K}(\mathbf{x}), \end{aligned} \tag{4}$$

where the macroscopic quantities $\boldsymbol{\Sigma}(\mathbf{x})$ and $\mathbf{M}(\mathbf{x})$ are the asymmetric stress tensor and the couple stress tensor, respectively, and $\mathbb{G}^M = G_{ijhk}\mathbf{e}_i \otimes \mathbf{e}_j \otimes \mathbf{e}_h \otimes \mathbf{e}_k$, $\mathbf{Y}^M = Y_{ijh}\mathbf{e}_i \otimes \mathbf{e}_j \otimes \mathbf{e}_h$, $\mathbf{Y}^{M^T} = Y_{ijh}\mathbf{e}_h \otimes \mathbf{e}_i \otimes \mathbf{e}_j$ and $\mathbf{S}^M = S_{ij}\mathbf{e}_i \otimes \mathbf{e}_j$ are the macroscopic homogeneous constitutive tensors. The balance of momentum and balance of moment of momentum result

$$\begin{aligned} &\nabla \cdot \boldsymbol{\Sigma}(\mathbf{x}) + \mathbf{b}(\mathbf{x}) = \mathbf{0}, \\ &\nabla \cdot \mathbf{M}(\mathbf{x}) - \varepsilon_{3ij}(\mathbf{e}_i \otimes \mathbf{e}_j) : \boldsymbol{\Sigma}(\mathbf{x}) + c_3(\mathbf{x}) = \mathbf{0}, \end{aligned} \tag{5}$$

where $\mathbf{b}(\mathbf{x})$ and $c_3(\mathbf{x})$ are the body forces and the body couples, respectively.
By exploiting the balance equations (5), recalling the constitutive equations (4) and the definitions of asymmetric micropolar strain tensor $\boldsymbol{\Gamma}(\mathbf{x})$ and curvature tensor $\mathbf{K}(\mathbf{x})$, the governing equation in terms of the components of the generalized displacements $\mathbf{U}(\mathbf{x})$ and $\Phi(\mathbf{x})$ takes the following form

$$\begin{aligned}
&\nabla \cdot \left[\mathbb{G}^M \left(\nabla \mathbf{U}(\mathbf{x}) + \varepsilon_{3hk} \left(\mathbf{e}_h \otimes \mathbf{e}_k\right) \Phi\left(\mathbf{x}\right)\right)\right] + \nabla \cdot \left(\mathbf{Y}^M \nabla \Phi(\mathbf{x})\right) + \mathbf{b}(\mathbf{x}) = \mathbf{0}, \\
&\nabla \cdot \left[\mathbf{Y}^{M^T} \left(\nabla \mathbf{U}(\mathbf{x}) + \varepsilon_{3hk} (\mathbf{e}_h \otimes \mathbf{e}_k) \Phi(\mathbf{x})\right)\right] + \nabla \cdot \left(\mathbf{S}^M \nabla \Phi(\mathbf{x})\right) + \\
&- \varepsilon_{3ij} (\mathbf{e}_i \otimes \mathbf{e}_j) : \left[\mathbb{G}^M \left(\nabla \mathbf{U}(\mathbf{x}) + \varepsilon_{3hk} (\mathbf{e}_h \otimes \mathbf{e}_k) \Phi(\mathbf{x})\right) + \mathbf{Y}^M \nabla \Phi(\mathbf{x})\right] + c_3(\mathbf{x}) = 0.
\end{aligned} \tag{6}$$

Concerning the body couples, without loss of generality, in the following $c_3(\mathbf{x}) = 0$ will be considered.

3. Outline of the proposed method

The proposed homogenization technique consists of three successive steps, which are detailed in the following sub-paragraphs. Firstly in subsection 3.1, the standard homogenization scheme is applied in order to determine both the perturbation functions, characterizing the geometric and mechanical properties of the periodic microstructure, as well as the overall constitutive tensor of the first order equivalent continuum. Secondly in subsection 3.2, based on the results of the previous step, the upscaling relations, defining the macroscopic generalized displacements in terms of the microscopic displacement field, are properly established. In addition, the kinematic map, which describes the microscopic displacement field explicitly dependent on macroscopic constants associated with the micropolar deformation modes, is uniquely defined. Finally in subsection 3.3, the generalized macro-homogeneity condition is introduced to identify, in closed form, the overall elastic constitutive equations characterizing the equivalent micropolar continuum, that directly descend from the heterogeneous microstructure through the perturbation functions.

3.1. Micro-macro kinematic relations and asymptotic expansion of the microscopic governing equations

In order to define the kinematic relations between the two scales, i.e. upscaling and downscaling relations that will be fully developed in the following subsection 3.2, the microscopic displacement field is here represented via an asymptotic expansion in terms of the microstructural length ε. The idea is to describe the microscopic displacement field as the superposition of a macroscopic displacement field and a properly defined microscopic displacement fluctuation field. This latter field depends, in turn, on gradients of the macroscopic displacement field, as well as on periodic perturbation functions. In particular, the asymptotic expansion takes the following form as in [5, 13, 15]

$$\begin{aligned}
u_i\left(\mathbf{x}, \xi = \frac{\mathbf{x}}{\varepsilon}\right) &= \left(u_i^*(\mathbf{x}) + \sum_{l=1}^{+\infty} \varepsilon^l \sum_{|q|=l} N_{ijq}^{(l)}(\boldsymbol{\xi}) \frac{\partial^{|q|}}{\partial x_q} u_j^*(\mathbf{x})\right)\Bigg|_{\xi=\frac{\mathbf{x}}{\varepsilon}} = \\
&= \left(u_i^*(\mathbf{x}) + \varepsilon N_{ijq_1}^{(1)}(\boldsymbol{\xi}) \frac{\partial u_j^*(\mathbf{x})}{\partial x_{q_1}} + \varepsilon^2 N_{ijq_1q_2}^{(2)}(\boldsymbol{\xi}) \frac{\partial^2 u_j^*(\mathbf{x})}{\partial x_{q_1} \partial x_{q_2}} + \right. \\
&\left. + \varepsilon^3 N_{ijq_1q_2q_3}^{(3)}(\boldsymbol{\xi}) \frac{\partial^3 u_j^*(\mathbf{x})}{\partial x_{q_1} \partial x_{q_2} \partial x_{q_3}} + \mathcal{O}\left(\varepsilon^4\right)\right)\Bigg|_{\xi=\frac{\mathbf{x}}{\varepsilon}},
\end{aligned} \tag{7}$$

where $u_i^*(\mathbf{x})$ are $\mathcal{L}$-periodic functions depending on the slow variable $\mathbf{x}$, $N_{ijq}^{(l)}$ are Q-periodic perturbation functions depending on the fast variable $\xi = \frac{\mathbf{x}}{\varepsilon}$, that are characterized by zero mean value within the unit cell Q, i.e. $\int_Q N_{ijq}^l(\boldsymbol{\xi})\, d\boldsymbol{\xi} = 0$ (so called *normalization condition*), and vanish for homogeneous microstructure, and finally $q = q_1, ..., q_l$ is a multi-index, with $|q|$ being the multi-index length and $\frac{\partial^l}{\partial x_q}(\cdot) = \frac{\partial^l}{\partial x_1 ... \partial x_l}(\cdot)$.

It is possible to define the macro-displacement field by averaging the microscopic displacement field within the unit cell $\mathcal{Q}$, that is

$$U_i(\mathbf{x}) = \int_{\mathcal{Q}} \left(u_i^*(\mathbf{x}) + \sum_{l=1}^{+\infty} \varepsilon^l \sum_{|q|=l} N_{ijq}^{(l)}(\boldsymbol{\xi}+\boldsymbol{\zeta}) \frac{\partial^{|q|}}{\partial x_q} u_j^*(\mathbf{x}) \right)\Bigg|_{\xi=\frac{\mathbf{x}}{\varepsilon}} d\boldsymbol{\zeta}, \tag{8}$$

where $\boldsymbol{\zeta} \in \mathcal{Q}$ is a *translation variable*, such that the vector $\varepsilon\boldsymbol{\zeta} \in \mathcal{A}$ defines a translation of the heterogeneous medium with respect to fixed $\mathcal{L}$-periodic body forces $\mathbf{b}(\mathbf{x})$ [11, 15]. It is pointed out that, in equation (8), the perturbation functions fulfill the invariance property satisfied by $\mathcal{Q}$-periodic functions $g(\boldsymbol{\xi}+\boldsymbol{\zeta})|_{\xi=\frac{\mathbf{x}}{\varepsilon}}$, such that $\int_{\mathcal{Q}} g(\frac{\mathbf{x}}{\varepsilon}+\boldsymbol{\zeta})d\boldsymbol{\zeta} = \int_{\mathcal{Q}} g(\boldsymbol{\xi}+\boldsymbol{\zeta})d\boldsymbol{\zeta} = \int_{\mathcal{Q}} g(\boldsymbol{\xi}+\boldsymbol{\zeta})d\boldsymbol{\xi}$. By exploiting this property and the *normalization condition*, the equivalence is recovered as $U_i(\mathbf{x}) = u_i^*$. By plugging this relation into equation (7), the final form of the downscaling relations is obtained

$$u_i\left(\mathbf{x}, \xi = \frac{\mathbf{x}}{\varepsilon}\right) = \left(U_i(\mathbf{x}) + \sum_{l=1}^{+\infty} \varepsilon^l \sum_{|q|=l} N_{ijq}^{(l)}(\boldsymbol{\xi}) \frac{\partial^{|q|}}{\partial x_q} U_j(\mathbf{x}) \right)\Bigg|_{\xi=\frac{\mathbf{x}}{\varepsilon}}. \tag{9}$$

Moreover, recalling the derivation rule valid for the function $f\left(\mathbf{x}, \boldsymbol{\xi} = \frac{\mathbf{x}}{\varepsilon}\right)$, that is

$$\frac{D}{Dx_j} f\left(\mathbf{x}, \boldsymbol{\xi} = \frac{\mathbf{x}}{\varepsilon}\right) = \left(\frac{\partial f}{\partial x_j} + \frac{1}{\varepsilon} \frac{\partial f}{\partial \xi_j} \right)\Bigg|_{\boldsymbol{\xi}=\frac{\mathbf{x}}{\varepsilon}} = \left(\frac{\partial f}{\partial x_j} + \frac{1}{\varepsilon} f_{,j} \right)\Bigg|_{\boldsymbol{\xi}=\frac{\mathbf{x}}{\varepsilon}}, \tag{10}$$

the equation (9) can be, thus, plug into the microscopic governing equation (1) and the related interface conditions (2). After suitable manipulations, by collecting the terms with equal power ε, and imposing the solvability condition in the class of $\mathcal{Q}$-periodic functions, a hierarchical sequence of partial differential problems, known as *cell problems*, is obtained. More specifically, the differential problems, expressed in terms of the perturbation functions $N_{ijq}^{(l)}$, are characterized by zero mean value of source terms in the unit cell $\mathcal{Q}$. Therefore, they admit sufficiently regular and $\mathcal{Q}$-periodic solutions, for details see [13, 15]. The uniqueness of solution is, finally, obtained through the *normalization condition* which ensures the zero mean value of perturbation functions within the unit cell $\mathcal{Q}$.
Therefore, the *cell problem* at the order ε^{-1} reads

$$\left(C_{ijhk}^m N_{hpq_1,k}^{(1)} \right)_{,j} + C_{ijpq_1,j}^m = 0, \tag{11}$$

and the related interface and *normalization conditions* are

$$\begin{aligned} &\left[\left[N_{hpq_1}^{(1)} \right]\right]\Big|_{\boldsymbol{\xi}\in\Gamma_1} = 0, \\ &\left[\left[C_{ijhk}^m \left(\delta_{hp}\delta_{kq_1} + N_{hpq_1,k}^{(1)} \right) n_j \right]\right]\Big|_{\boldsymbol{\xi}\in\Gamma_1} = 0, \\ &\int_{\mathcal{Q}} N_{ijq_1}^{(1)} d\boldsymbol{\xi} = 0, \end{aligned} \tag{12}$$

where Γ_1 is the interface between two different phases in the unit cell $\mathcal{Q}$, and δ_{ij} is the Kronecker delta function.
Analogously, the *cell problem* at the order ε^0 is

$$\begin{aligned} &\left(C_{ijhk}^m N_{hpq_1q_2,k}^{(2)} \right)_{,j} + \frac{1}{2}\left[\left(C_{ijhq_2}^m N_{hpq_1}^{(1)} + C_{ijhq_1}^m N_{hpq_2}^{(1)} \right)_{,j} + C_{iq_1hk}^m N_{hpq_2,k}^{(1)} + C_{iq_1pq_2}^m + \right. \\ &\left. + C_{iq_2hk}^m N_{hpq_1,k}^{(1)} + C_{iq_2pq_1}^m \right] = \frac{1}{2} \int_{\mathcal{Q}} \left(C_{iq_1hk}^m N_{hpq_2,k}^{(1)} + C_{iq_1pq_2}^m + C_{iq_2hk}^m N_{hpq_1,k}^{(1)} + C_{iq_2pq_1}^m \right) d\boldsymbol{\xi}, \end{aligned} \tag{13}$$

and the related interface and *normalization conditions* are

$$\begin{aligned}
&\left[\left[N^{(2)}_{hpq_1q_2}\right]\right]\Big|_{\boldsymbol{\xi}\in\Gamma_1} = 0,\\
&\left[\left[\left\{C^m_{ijhk}N^{(2)}_{hpq_1q_2,k} + \frac{1}{2}\left(C^m_{ijhq_2}N^{(1)}_{hpq_1} + C^m_{ijhq_1}N^{(1)}_{hpq_2}\right)\right\}n_j\right]\right]\Big|_{\boldsymbol{\xi}\in\Gamma_1} = 0,\\
&\int_Q N^{(2)}_{hpq_1q_2}d\boldsymbol{\xi} = 0,
\end{aligned} \tag{14}$$

Finally, the generic *cell problem* at the order ε^m (for $m \in \mathbb{Z}$, $m \geq 1$) takes the following form

$$\begin{aligned}
&\left(C^m_{ijhk}N^{(m+2)}_{hpq_1..q_{m+2},k}\right)_{,j} + \frac{1}{m+2}\sum_{\wp^*(q)}\left[\left(C^m_{ijhq_{m+2}}N^{(m+1)}_{hpq_1..q_{m+1},k}\right)_{,j} + C^m_{iq_{m+1}hq_{m+2}}N^{(m)}_{hpq_1...q_m} + \right.\\
&\left.+C^m_{iq_{m+2}hk}N^{(m)}_{hpq_1...q_{m+1},k}\right] = \frac{1}{m+2}\sum_{\wp^*(q)}\int_Q\left(C^m_{iq_{m+1}hq_{m+2}}N^{(m)}_{hpq_1...q_m} + C^m_{iq_{m+2}hk}N^{(m)}_{hpq_1...q_{m+1},k}\right)d\boldsymbol{\xi},
\end{aligned} \tag{15}$$

and the associated interface and *normalization conditions* are

$$\begin{aligned}
&\left[\left[N^{(m+2)}_{hpq_1...q_{m+2}}\right]\right]\Big|_{\boldsymbol{\xi}\in\Gamma_1} = 0,\\
&\left[\left[\left\{C^m_{ijhk}\left[N^{(m+2)}_{hpq_1...q_{m+2},k} + \frac{1}{m+2}\sum_{\wp^*(q)}\left(\delta_{q_{m+2}k}N^{(m+1)}_{hpq_1...q_{m+1}}\right)\right]\right\}n_j\right]\right]\Big|_{\boldsymbol{\xi}\in\Gamma_1} = 0,\\
&\int_Q N^{(m+2)}_{hpq_1...q_{m+2}}d\boldsymbol{\xi} = 0,
\end{aligned} \tag{16}$$

where $\delta_{q_{m+2}k}$ is the Kronecker delta function, and $\wp^*(q)$ denotes all the possible permutations of the multi-index q, such that if $|q| = m+2$, it follows that

$$\begin{aligned}
\wp^*(q) = \{&f_1 = (q_1 \to q_1, q_2 \to q_2, ..., q_{m+2} \to q_{m+2}),\ ...,\\
&f_{m+2} = (q_1 \to q_{m+2}, q_2 \to q_1, ..., q_{m+2} \to q_2)\},
\end{aligned}$$

with f_i, i=1,.., $m+2$, being index permutation functions. In particular, in the *cell problem* at order ε, obtained by replacing m=1 in equations (15) and (16) with solution in terms of the perturbation functions $N^{(3)}_{ijq_1q_2q_3}$, it reads $|q| = 3$, and

$$\begin{aligned}
\wp^*(q) = \{&f_1 = (q_1 \to q_1, q_2 \to q_2, q_3 \to q_3), f_2 = (q_1 \to q_2, q_2 \to q_3, q_3 \to q_1),\\
&f_3 = (q_1 \to q_3, q_2 \to q_1, q_3 \to q_2)\}.
\end{aligned}$$

By solving the hierarchical *cell problems*, the perturbation functions $N^{(l)}_{ijq}$ are determined. Consequently, the governing equations at the microscopic scale, equation (1), after performing asymptotic expansion and exploiting the solvability conditions, result in fully determined average field equations of infinite order. In particular, these equations are expressed in terms of both the macroscopic field, that is only dependent on the *slow* variable $\mathbf{x}$, and on homogeneous overall tensors. The average field equations of infinite order are thus

$$n^{(2)}_{ipq_1q_2}\frac{\partial^2 U_p(\mathbf{x})}{\partial x_{q_1}\partial x_{q_2}} + \sum_{m=1}^{+\infty}\varepsilon^m\sum_{|q|=m+2}n^{(m+2)}_{ipq}\frac{\partial^{m+2}U_p(\mathbf{x})}{\partial x_q} + b_i(\mathbf{x}) = 0, \tag{17}$$

where the coefficients $n^{(2)}_{ipq_1q_2}$ and $n^{(m+2)}_{ipq}$ are

$$\begin{aligned} n^{(2)}_{ipq_1q_2} &= \frac{1}{2}\int_{Q}\left(C^{m}_{iq_1hk}N^{(1)}_{hpq_2,k} + C^{m}_{iq_1pq_2} + C^{m}_{iq_2hk}N^{(1)}_{hpq_1,k} + C^{m}_{iq_2pq_1}\right)d\boldsymbol{\xi}, \\ n^{(m+2)}_{ipq} &= \frac{1}{m+2}\sum_{\wp^*(q)}\int_{Q}\left(C^{m}_{iq_{m+1}hq_{m+2}}N^{(m)}_{hpq_1\dots q_m} + C^{m}_{iq_{m+2}hk}N^{(m)}_{hpq_1\dots q_{m+1},k}\right)d\boldsymbol{\xi}. \end{aligned} \tag{18}$$

The equation (17) can be formally solved by performing an asymptotic expansion of the macrofield $U_i(\mathbf{x})$, in power series of ε, that is

$$U_i(\mathbf{x}) = \sum_{j=0}^{+\infty}\varepsilon^j U_i^{(j)}(\mathbf{x}). \tag{19}$$

Therefore, by plugging equations (19) into equations (17), a sequence of partial differential equations in terms of the macroscopic fields $U_i^{(j)}(\mathbf{x})$ is obtained. At the order ε^0, the following macro-problems holds

$$n^{(2)}_{ipq_1q_2}\frac{\partial^2 U_p^{(0)}}{\partial x_{q_1}\partial x_{q_2}} + b_i(\mathbf{x}) = 0, \tag{20}$$

while at the order ε^m (with $m \in \mathbb{Z}$ and $m > 1$) it results

$$n^{(2)}_{ipq_1q_2}\frac{\partial^2 U_p^{(m)}}{\partial x_{q_1}\partial x_{q_2}} + \sum_{r=3}^{m+2}\sum_{|j|=r} n^{(r)}_{ipj}\frac{\partial^r U_p^{(m-r+2)}}{\partial x_j} = 0. \tag{21}$$

In the particular case of the macroscopic displacement field truncated at order 0-th, i.e. $U_i(\mathbf{x}) \approx U_i^0(\mathbf{x})$, the equation (20) specializes in the following form

$$n^{(2)}_{ipq_1q_2}\frac{\partial^2 U_p(\mathbf{x})}{\partial x_{q_1}\partial x_{q_2}} + b_i(\mathbf{x}) = 0. \tag{22}$$

Analogously to [13], it is possible to prove that equation (22) can be arranged in an equivalent form in terms of the components of the macroscopic elastic tensor $C_{iq_2pq_1}$ of a first order homogeneous linear elastic continuum, by exploiting the relation $n^{(2)}_{ipq_1q_2} = \frac{1}{2}\left(C_{iq_1pq_2} + C_{iq_2pq_1}\right)$.
Moreover, due to the repetition of indices q_1 and q_2, it results

$$\begin{aligned} n^{(2)}_{ipq_1q_2}\frac{\partial^2 U_p(\mathbf{x})}{\partial x_{q_1}\partial x_{q_2}} &= \frac{1}{2}\left(C_{iq_1pq_2} + C_{iq_2pq_1}\right)\frac{\partial^2 U_p(\mathbf{x})}{\partial x_{q_1}\partial x_{q_2}} = \\ &= \frac{1}{2}\left(C_{pq_1iq_2}\frac{\partial^2 U_p(\mathbf{x})}{\partial x_{q_1}\partial x_{q_2}} + C_{iq_2pq_1}\frac{\partial^2 U_p(\mathbf{x})}{\partial x_{q_1}\partial x_{q_2}}\right) = C_{iq_2pq_1}\frac{\partial^2 U_p(\mathbf{x})}{\partial x_{q_1}\partial x_{q_2}}, \end{aligned} \tag{23}$$

therefore the final form of equation (22) is

$$C_{iq_2pq_1}\frac{\partial^2 U_p(\mathbf{x})}{\partial x_{q_1}\partial x_{q_2}} + b_i(\mathbf{x}) = 0, \tag{24}$$

where the components of the macroscopic elastic tensor of the first order homogeneous continuum are expressed in terms of the perturbation function $N^{(1)}_{kpq_1}$ and take the form

$$C_{iq_2pq_1} = \int_{Q} C^{m}_{rjkl}\left(N^{(1)}_{riq_2,j} + \delta_{ir}\delta_{jq_2}\right)\left(N^{(1)}_{kpq_1,l} + \delta_{pk}\delta_{lq_1}\right)d\boldsymbol{\xi}. \tag{25}$$

It is, finally, pointed out that the macroscopic elastic tensor satisfies both the positive definiteness and major and minor symmetries, i.e. $C_{pq_1iq_2} = C_{iq_2pq_1}$, $C_{pq_1iq_2} = C_{q_1piq_2} = C_{q_1pq_2i} = C_{pq_1q_2i}$. Moreover, the field equations (22) and (24) are elliptic. These properties descend from the positive definiteness, from major and minor symmetries of the microscopic elastic tensor components C^m_{rjkl}, and from the equality $N^{(1)}_{kpq_1} = N^{(1)}_{kq_1p}$ whose validity is guaranteed by the structure of the cell problem (11) and (12).
Higher-order governing equations can be analogously derived by truncating the macroscopic displacement field, equation (19), at order m-th ($m > 0$). In this case, the governing equations depend on both overall first order tensors and on so-called auxiliary volume forces. Such volume forces depend, in turn, on higher order overall constitutive tensors and on previous orders solutions. Adopting these volume forces, it is, moreover, possible to account for nonlocal effects occurring in average field equations of infinite order, that result asymptotically equivalent to the field equations governing the heterogeneous material, see for details [51]. As the approximation order increases, a better estimation of the actual heterogeneous medium solution is, indeed, obtained.

3.2. Upscaling relations and third order polynomial kinematic map

The upscaling relations, linking the generalized macro-displacement field, depending on both $\mathbf{U}(\mathbf{x})$ and $\Phi(\mathbf{x})$, to the displacement field at the microscopic level $\mathbf{u}(\mathbf{x})$, are here discussed. Regarding the continuum field $\mathbf{U}(\mathbf{x})$, the following standard expressions derive from equation (8) as

$$\begin{aligned} U_1(\mathbf{x}) &= \int_Q u_1(\mathbf{x}, \boldsymbol{\xi}) d\boldsymbol{\xi}, \\ U_2(\mathbf{x}) &= \int_Q u_2(\mathbf{x}, \boldsymbol{\xi}) d\boldsymbol{\xi}. \end{aligned} \tag{26}$$

On the other hand, concerning the micropolar rotation field $\Phi(\mathbf{x})$, a newly proposed upscaling relation is introduced. The idea is to exploit a minimization procedure over the unit cell Q to find the components of the skew-symmetric micropolar rotation tensor that best fit the micro infinitesimal rotation tensor of the actual heterogeneous medium.
Recalling the relation $W_{ij} = -\varepsilon_{3ij}\Phi$, indeed, the following least square minimization procedure is exploited

$$\begin{aligned} \min_{W_{ij}} \mathcal{F}\left[\omega^*_{ij}(W_{ij})\right] &= \min_{W_{ij}} \int_Q \left(\|\omega_{ij}(\mathbf{x}, \frac{\mathbf{x}}{\varepsilon} + \boldsymbol{\zeta}) - \omega^*_{ij}(\mathbf{x}, \frac{\mathbf{x}}{\varepsilon} + \boldsymbol{\zeta})\|_2 \right)^2 d\boldsymbol{\zeta} = \\ &= \min_{W_{ij}} \int_Q \left(\|\omega_{ij}(\mathbf{x}, \boldsymbol{\xi}) - \omega^*_{ij}(\mathbf{x}, \boldsymbol{\xi})\|_2 \right)^2 d\boldsymbol{\xi}, \end{aligned} \tag{27}$$

where the symbol $\|\cdot\|_2$ is the Euclidean norm, and ω_{ij} are the components of the micro infinitesimal rotation tensor, depending both on the *slow* variable $\mathbf{x}$ and the *fast* variable $\boldsymbol{\xi}$, as

$$\omega_{ij}\left(\mathbf{x}, \boldsymbol{\xi} = \frac{\mathbf{x}}{\varepsilon}\right) = \frac{1}{2}\left(\frac{Du_i}{Dx_j} - \frac{Du_j}{Dx_i}\right) = \frac{1}{2}\left(\frac{\partial u_i}{\partial x_j} - \frac{\partial u_j}{\partial x_i} + \frac{1}{\varepsilon}\left(u_{i,j} - u_{j,i}\right)\right)\Bigg|_{\boldsymbol{\xi}=\frac{\mathbf{x}}{\varepsilon}}, \tag{28}$$

it follows that

$$\omega_{ij}(\mathbf{x}, \boldsymbol{\xi}) = \frac{1}{2}\left(\frac{\partial u_i}{\partial x_j} - \frac{\partial u_j}{\partial x_i} + \frac{1}{\varepsilon}\left(u_{i,j} - u_{j,i}\right)\right). \tag{29}$$

Moreover, in equation (27), ω^*_{ij} are the components of a properly defined skew-symmetric tensor, depending on the components of both the micropolar rotation tensor W_{ij} and the perturbation functions $N^{(l)}_{ijk}$, that

take the following form

$$\begin{aligned}\omega_{ij}^{*} =& W_{ij} + \sum_{l=1}^{+\infty} \sum_{\substack{|q|=l \\ |r|=l}} \frac{1}{2} \left(N_{ijq,r}^{(l)} - N_{jiq,r}^{(l)} \right) \tilde{W}_{qr} = \\ =& W_{ij} + \frac{1}{2} \left(N_{ijq_1,r_1}^{(1)} - N_{jiq_1,r_1}^{(1)} \right) \tilde{W}_{q_1 r_1} + \frac{1}{2} \left(N_{ijq_1q_2,r_1r_2}^{(2)} - N_{jiq_1q_2,r_1r_2}^{(2)} \right) \tilde{W}_{q_1q_2r_1r_2} + \\ &+ \ldots\ldots + \frac{1}{2} \left(N_{ijq_1q_2\ldots q_n,r_1r_2\ldots r_n}^{(n)} - N_{jiq_1q_2\ldots q_n,r_1r_2\ldots r_n}^{(n)} \right) \tilde{W}_{q_1q_2\ldots q_nr_1r_2\ldots r_n} + \ldots\ldots,\end{aligned} \tag{30}$$

where $\tilde{W}_{q_1r_1} = W_{q_1r_1}$, $\tilde{W}_{q_1q_2r_1r_2} = W_{q_1r_2}\delta_{q_2r_1}$, and $\tilde{W}_{q_1q_2\ldots q_nr_1r_2\ldots r_n} = W_{q_1r_n}\delta_{q_2r_1}\ldots\delta_{q_nr_{n-1}}$, with $m \in \mathbb{Z}$, $n \geq 2$.
Considering only the first term of the series, it results

$$\omega_{ij}^{*}(\mathbf{x}, \boldsymbol{\xi}) \approx W_{ij} + \frac{1}{2} \left(N_{ijp,q_1}^{(1)} - N_{jip,q_1}^{(1)} \right) W_{pq_1} = \left[\delta_{ip}\delta_{jq_1} + \frac{1}{2} \left(N_{ijp,q_1}^{(1)} - N_{jip,q_1}^{(1)} \right) \right] W_{pq_1}, \tag{31}$$

where exclusively first order perturbation functions appear. Substituting equations (29) and (31) into equation (27), after solving the minimization problem, the components of the micropolar rotation tensor are obtained as

$$W_{ij}(\mathbf{x}) = \frac{\int_Q \omega_{pq_1}(\mathbf{x}, \boldsymbol{\xi}) \left[\delta_{ip}\delta_{jq_1} + \frac{1}{2} \left(N_{ijp,q_1}^{(1)} - N_{jip,q_1}^{(1)} \right) \right] d\boldsymbol{\xi}}{\int_Q \delta_{pr}\delta_{q_1s_1} \left[\delta_{hp}\delta_{kq_1} + \frac{1}{2} \left(N_{hkp,q_1}^{(1)} - N_{jhp,q_1}^{(1)} \right) \right] \left[\delta_{hr}\delta_{ks_1} + \frac{1}{2} \left(N_{hkr,s_1}^{(1)} - N_{khr,s_1}^{(1)} \right) \right] d\boldsymbol{\xi}}. \tag{32}$$

Finally, the expression of the micropolar rotation tensor $\Phi(\mathbf{x})$ is found by specializing equation (32) as

$$\Phi(\mathbf{x}) = W_{21}(\mathbf{x}) = \frac{\int_Q \omega_{21}(\mathbf{x}, \boldsymbol{\xi}) \left[1 + \frac{1}{2} \left(N_{121,2}^{(1)} - N_{211,2}^{(1)} - N_{122,1}^{(1)} + N_{212,1}^{(1)} \right) \right] d\boldsymbol{\xi}}{\int_Q \left[1 + \frac{1}{2} \left(N_{121,2}^{(1)} - N_{211,2}^{(1)} - N_{122,1}^{(1)} + N_{212,1}^{(1)} \right) \right]^2 d\boldsymbol{\xi}}, \tag{33}$$

where the component ω_{21} of the micro infinitesimal rotation tensor is obtained through equation (29).
The upscaling relations, equations (26) and (33), are now particularized to the case in which the microscopic displacement field $u_i(\mathbf{x}, \boldsymbol{\xi})$ is described by the asymptotic expansion (9) properly truncated. In particular, only the first three terms of the series are retained, resulting in

$$u_i^{III}(\mathbf{x}, \boldsymbol{\xi}) = U_i(\mathbf{x}) + \varepsilon N_{ijq_1}^{(1)}(\boldsymbol{\xi}) H_{jq_1}(\mathbf{x}) + \varepsilon^2 N_{ijq_1q_2}^{(2)}(\boldsymbol{\xi}) \kappa_{jq_1q_2}(\mathbf{x}) + \varepsilon^3 N_{ijq_1q_2q_3}^{(3)}(\boldsymbol{\xi}) \kappa_{jq_1q_2q_3}(\mathbf{x}), \tag{34}$$

where the macroscopic fields $U_i(\mathbf{x})$, $H_{jq_1}(\mathbf{x})$, $\kappa_{jq_1q_2}(\mathbf{x})$ and $\kappa_{jq_1q_2q_3}(\mathbf{x})$ are detailed in the following. It is worth mentioning that the microscopic displacement field is defined by superposing the macro-displacement field and a combination of fluctuating fields within the unit cell that are obtained by solving the nested *cell problems* presented in subsection 3.1.
Concerning the macro-displacement, a third-order Taylor polynomial expansion is chosen

$$U_i(\mathbf{x}) = \bar{U}_i + \bar{H}_{ip_1}x_{p_1} + \frac{1}{2}\bar{\kappa}_{ip_1p_2}x_{p_1}x_{p_2} + \frac{1}{6}\bar{\kappa}_{ip_1p_2p_3}x_{p_1}x_{p_2}x_{p_3}, \tag{35}$$

where $\bar{U}_i$, $\bar{H}_{ip_1}$, $\bar{\kappa}_{ip_1p_2}$ and $\bar{\kappa}_{ip_1p_2p_3}$ are the macro-displacement components, and the first, the second and the third displacement gradient components evaluated at point $\mathbf{x} = \mathbf{0}$, respectively. Particularly, the equation (35) contains 20 independent coefficients that can be reduced to 6, accordingly with [34], by applying the set of hypotheses discussed here below.
As a first assumption, the components of the macro-displacement evaluated at point $\mathbf{x} = \mathbf{0}$ vanish, i.e. $\bar{U}_i = 0$. Moreover, the components of the skew-symmetric part of the displacement gradient, evaluated in

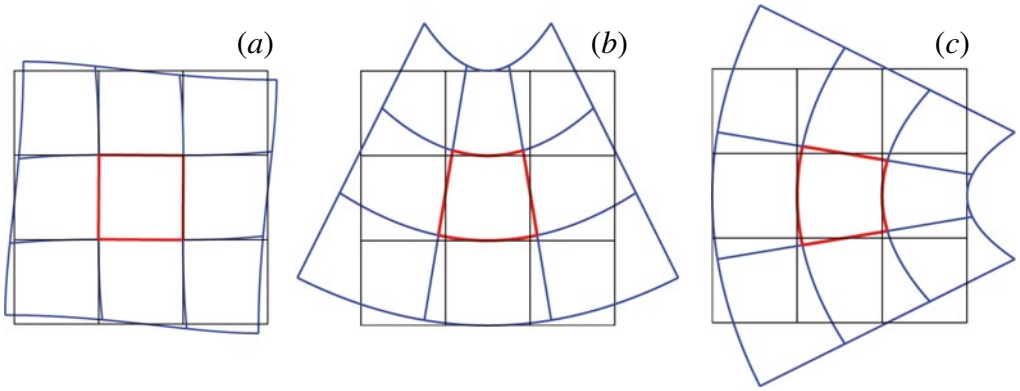

Figure 2: Selected micropolar deformation modes: mode associated to (a) $\bar{\kappa}_{1222}$; (b) $\bar{\kappa}_{122}$ and (c) $\bar{\kappa}_{211}$.

$\mathbf{x} = \mathbf{0}$, is set equal to zero, namely $\bar{\Omega}_{ij} = 0$ and, therefore, $\bar{H}_{ij} = \bar{E}_{ij}$, with $\bar{E}_{ij}$ being the components of the symmetric part of the displacement gradient in $\mathbf{x} = \mathbf{0}$. Besides, analogously to [23, 42, 50], it is assumed that the macroscopic displacement field $\mathbf{U}(\mathbf{x})$, expressed in equation (35), satisfies the field equations of an equivalent homogeneous first order continuum in the absence of body forces, i.e. $\nabla \cdot (\mathbb{C}\nabla\mathbf{U}(\mathbf{x})) = \mathbf{0}$, where $\mathbb{C}{=}C_{ijhk}\mathbf{e}_i \otimes \mathbf{e}_j \otimes \mathbf{e}_h \otimes \mathbf{e}_k$ is the overall elasticity tensor, obtained through equation (25). As a consequence, the coefficients $\bar{\kappa}_{ip_1p_2}$ and $\bar{\kappa}_{ip_1p_2p_3}$ of (35) must fulfill a set of 6 algebraic equations. Without loss of generality, the particular case of orthotropic material symmetry is here considered, thus these algebraic equations assume the following form

$$\begin{aligned}
&C_{\alpha\alpha\alpha\alpha}\bar{\kappa}_{\alpha\alpha\alpha} + C_{\alpha\beta\alpha\beta}\bar{\kappa}_{\alpha\beta\beta} + (C_{\alpha\alpha\beta\beta} + C_{\alpha\beta\alpha\beta})\bar{\kappa}_{\beta\alpha\beta} = 0,\\
&C_{\alpha\alpha\alpha\alpha}\bar{\kappa}_{\alpha\alpha\alpha\alpha} + C_{\alpha\beta\alpha\beta}\bar{\kappa}_{\alpha\alpha\beta\beta} + (C_{\alpha\alpha\beta\beta} + C_{\alpha\beta\alpha\beta})\bar{\kappa}_{\beta\beta\alpha\alpha} = 0,\\
&C_{\alpha\alpha\alpha\alpha}\bar{\kappa}_{\alpha\beta\alpha\alpha} + C_{\alpha\beta\alpha\beta}\bar{\kappa}_{\alpha\beta\beta\beta} + (C_{\alpha\alpha\beta\beta} + C_{\alpha\beta\alpha\beta})\bar{\kappa}_{\beta\alpha\beta\beta} = 0,
\end{aligned} \tag{36}$$

where the indices α, β are not summed up and it is assumed that $\alpha \neq \beta$ with $\alpha,\beta = 1, 2$. Finally, proper micropolar deformation modes are selected (as shown in Figure 2), so that $\kappa_{\alpha\alpha\alpha} = 0$; $\kappa_{\alpha\alpha\alpha\alpha} = 0$ and $\kappa_{\alpha\beta\beta\beta} = -\kappa_{\beta\alpha\alpha\alpha}$, with $\alpha \neq \beta$ and $\alpha,\beta = 1, 2$. Therefore, the resulting polynomial form of the macro-displacement components reads as

$$\begin{aligned}
U_\alpha(\mathbf{x}) = {}& \bar{E}_{\alpha\alpha}x_\alpha + \bar{E}_{\alpha\beta}x_\beta - \frac{C_{\alpha\beta\alpha\beta}}{C_{\alpha\alpha\beta\beta} + C_{\alpha\beta\alpha\beta}}\bar{\kappa}_{\beta\alpha\alpha}x_\alpha x_\beta + \frac{1}{2}\bar{\kappa}_{\alpha\beta\beta}x_\beta^2 + \frac{1}{6}\bar{\kappa}_{\alpha\beta\beta\beta}x_\beta^3 + \\
&- \frac{1}{2}\frac{C_{\alpha\beta\alpha\beta}\left[C_{\beta\beta\beta\beta}\bar{\kappa}_{\alpha\beta\beta\beta} - \left(C_{\alpha\alpha\beta\beta} + C_{\alpha\beta\alpha\beta}\right)\bar{\kappa}_{\beta\alpha\alpha\alpha}\right]}{C_{\alpha\alpha\alpha\alpha}C_{\beta\beta\beta\beta} - 2C_{\alpha\alpha\beta\beta}C_{\alpha\beta\alpha\beta} - \left(C_{\alpha\alpha\beta\beta}\right)^2 - \left(C_{\alpha\beta\alpha\beta}\right)^2},
\end{aligned} \tag{37}$$

where the indices α, β are not summed up and it is assumed that $\alpha \neq \beta$ with $\alpha,\beta = 1, 2$. This expression is also referred to as *kinematic map*. At this point, by replacing the equation (37) in (34), the polynomial approximation of the microscopic displacement field, in terms of $\bar{E}_{11}$, $\bar{E}_{22}$, $\bar{E}_{12}$, $\bar{\kappa}_{122}$, $\bar{\kappa}_{211}$, $\bar{\kappa}_{1222}$, takes the following form

$$\begin{aligned}
u_1(\mathbf{x},\boldsymbol{\xi}) = {}& \mathcal{B}_1^1(\mathbf{x},\boldsymbol{\xi})\,\bar{E}_{11} + \mathcal{B}_1^2(\mathbf{x},\boldsymbol{\xi})\,\bar{E}_{22} + \mathcal{B}_1^3(\mathbf{x},\boldsymbol{\xi})\,\bar{E}_{12} + \\
&+ \mathcal{B}_1^4(\mathbf{x},\boldsymbol{\xi})\,\bar{\kappa}_{122} + \mathcal{B}_1^5(\mathbf{x},\boldsymbol{\xi})\,\bar{\kappa}_{211} + \mathcal{B}_1^6(\mathbf{x},\boldsymbol{\xi})\,\bar{\kappa}_{1222},\\
u_2(\mathbf{x},\boldsymbol{\xi}) = {}& \mathcal{B}_2^1(\mathbf{x},\boldsymbol{\xi})\,\bar{E}_{11} + \mathcal{B}_2^2(\mathbf{x},\boldsymbol{\xi})\,\bar{E}_{22} + \mathcal{B}_2^3(\mathbf{x},\boldsymbol{\xi})\,\bar{E}_{12} + \\
&+ \mathcal{B}_2^4(\mathbf{x},\boldsymbol{\xi})\,\bar{\kappa}_{122} + \mathcal{B}_2^5(\mathbf{x},\boldsymbol{\xi})\,\bar{\kappa}_{211} + \mathcal{B}_2^6(\mathbf{x},\boldsymbol{\xi})\,\bar{\kappa}_{1222},
\end{aligned} \tag{38}$$

where the functions $\mathcal{B}_i^j(\mathbf{x},\boldsymbol{\xi})$ are reported in Appendix A.
By plugging equations (38) in equations (33) and (29), the micropolar rotation field $\Phi(\mathbf{x})$, is obtained. In

particular, the micropolar rotation evaluated in $\mathbf{x} = \mathbf{0}$, i.e. $\Phi^0 = \Phi(\mathbf{x} = \mathbf{0})$, results

$$\Phi^0 = \frac{\int_Q \left(C^1(\boldsymbol{\xi})\, \bar{E}_{11} + C^2(\boldsymbol{\xi})\, \bar{E}_{22} + C^3(\boldsymbol{\xi})\, \bar{E}_{12} + C^4(\boldsymbol{\xi})\, \bar{\kappa}_{122} + C^5(\boldsymbol{\xi})\, \bar{\kappa}_{211} + C^6(\boldsymbol{\xi})\, \bar{\kappa}_{1222} \right) d\boldsymbol{\xi}}{\int_Q (\Delta(\boldsymbol{\xi}))^2 d\boldsymbol{\xi}}, \tag{39}$$

with the functions $C^i(\boldsymbol{\xi})$ and $\Delta(\boldsymbol{\xi})$ being defined in Appendix A. Moreover, the components of the macroscopic curvature tensor $K_1 = \partial\Phi/\partial x_1$ and $K_2 = \partial\Phi/\partial x_2$, evaluated in $\mathbf{x} = \mathbf{0}$, i.e. $K_1^0 = K_1(\mathbf{x} = \mathbf{0})$ and $K_2^0 = K_2(\mathbf{x} = \mathbf{0})$ are

$$\begin{aligned} K_1^0 &= \frac{\int_Q \left(\mathcal{D}^1(\boldsymbol{\xi})\, \bar{\kappa}_{122} + \mathcal{D}^2(\boldsymbol{\xi})\, \bar{\kappa}_{211} + \mathcal{D}^3(\boldsymbol{\xi})\, \bar{\kappa}_{1222} \right) d\boldsymbol{\xi}}{\int_Q (\Delta(\boldsymbol{\xi}))^2 d\boldsymbol{\xi}}, \\ K_2^0 &= \frac{\int_Q \left(\mathcal{G}^1(\boldsymbol{\xi})\, \bar{\kappa}_{122} + \mathcal{G}^2(\boldsymbol{\xi})\, \bar{\kappa}_{211} + \mathcal{G}^3(\boldsymbol{\xi})\, \bar{\kappa}_{1222} \right) d\boldsymbol{\xi}}{\int_Q (\Delta(\boldsymbol{\xi}))^2 d\boldsymbol{\xi}}, \end{aligned} \tag{40}$$

where the functions $\mathcal{D}^i(\boldsymbol{\xi})$ and $\mathcal{G}^i(\boldsymbol{\xi})$ are, likewise, reported in Appendix A. Finally, the components of the asymmetric micropolar strain tensor, evaluated in $\mathbf{x} = \mathbf{0}$, i.e. $\Gamma_{ij}^0 = \Gamma_{ij}(\mathbf{x} = \mathbf{0})$ with $i, j = 1, 2$, read

$$\begin{aligned} \Gamma_{11}^0 &= \bar{E}_{11}, \\ \Gamma_{22}^0 &= \bar{E}_{22}, \\ \Gamma_{12}^0 &= \bar{E}_{12} + \Phi^0(\bar{E}_{11}, \bar{E}_{22}, \bar{E}_{12}, \bar{\kappa}_{122}, \bar{\kappa}_{211}, \bar{\kappa}_{1222}), \\ \Gamma_{21}^0 &= \bar{E}_{12} - \Phi^0(\bar{E}_{11}, \bar{E}_{22}, \bar{E}_{12}, \bar{\kappa}_{122}, \bar{\kappa}_{211}, \bar{\kappa}_{1222}), \end{aligned} \tag{41}$$

where, the following relations have been exploited,

$$\begin{aligned} \Gamma_{12}^0 &= \bar{E}_{12} + \bar{\Omega}_{12} - \bar{W}_{12} = \bar{E}_{12} + \bar{\Omega}_{12} + \Phi^0, \\ \Gamma_{21}^0 &= \bar{E}_{12} + \bar{\Omega}_{21} - \bar{W}_{21} = \bar{E}_{12} + \bar{\Omega}_{21} - \Phi^0, \end{aligned} \tag{42}$$

recalling that $\bar{\Omega}_{21} = -\bar{\Omega}_{12} = 0$, and $\bar{W}_{21} = -\bar{W}_{12} = \Phi^0$.

3.3. Generalized macro-homogeneity condition

The overall micropolar elastic properties are derived by exploiting a generalized macro-homogeneity condition, establishing an energy equivalence between the macroscopic and the microscopic scales. In what follows the matrix notation is used, consistently with the definitions in Appendix B.
Accordingly with [11, 15], the *microscopic mean strain energy* is defined as

$$\bar{\mathcal{E}}_m \doteq \frac{1}{2} \int_{\mathcal{A}} \int_Q \underline{\boldsymbol{\varepsilon}}(\mathbf{x}, \boldsymbol{\xi})^T\, \underline{\underline{\mathbf{C}}}^m(\boldsymbol{\xi})\, \underline{\boldsymbol{\varepsilon}}(\mathbf{x}, \boldsymbol{\xi})\, d\boldsymbol{\xi} d\mathbf{x}. \tag{43}$$

Under the assumption of scale separation, the macroscopic fields are both smooth and characterized by sufficiently small variations of the macroscopic variable $\mathbf{x}$ in the periodic cell $\mathcal{A}$. In this framework, the *microscopic mean strain energy* related to the strain field $\underline{\boldsymbol{\varepsilon}}$ evaluated in $\mathbf{x} = \mathbf{0}$ can be introduced as

$$\bar{\mathcal{E}}_m^0 \doteq \frac{1}{2} \int_{\mathcal{A}} \int_Q \underline{\boldsymbol{\varepsilon}}(\mathbf{x} = \mathbf{0}, \boldsymbol{\xi})^T\, \underline{\underline{\mathbf{C}}}^m(\boldsymbol{\xi})\, \underline{\boldsymbol{\varepsilon}}(\mathbf{x} = \mathbf{0}, \boldsymbol{\xi})\, d\boldsymbol{\xi} d\mathbf{x} = \frac{|\mathcal{A}|}{2} \int_Q \underline{\boldsymbol{\varepsilon}}_0^T \underline{\underline{\mathbf{C}}}^m \underline{\boldsymbol{\varepsilon}}_0 d\boldsymbol{\xi}, \tag{44}$$

where $|\mathcal{A}|$ corresponds to the area of the periodic cell, and $\underline{\boldsymbol{\varepsilon}}_0$ is the strain vector evaluated at $\mathbf{x} = \mathbf{0}$, i.e. $\underline{\boldsymbol{\varepsilon}}_0 = \underline{\boldsymbol{\varepsilon}}(\mathbf{x} = \mathbf{0}, \boldsymbol{\xi})$. This strain vector is determined from the microscopic displacement components in equation (38), by exploiting the derivation rule, reported in equation (10), and takes the form

$$\underline{\boldsymbol{\varepsilon}}_0 = \underline{\underline{\mathbf{B}}}^{\Xi}\underline{\boldsymbol{\Xi}} + \underline{\underline{\mathbf{B}}}^{\Upsilon}\underline{\boldsymbol{\Upsilon}}, \tag{45}$$

where the vectors $\underline{\boldsymbol{\Xi}}$ and $\underline{\boldsymbol{\Upsilon}}$ are expressed as

$$\underline{\boldsymbol{\Xi}} = \left\{ \begin{array}{cccc} \bar{E}_{11} & \bar{E}_{22} & \bar{E}_{12} & \bar{\kappa}_{1222} \end{array} \right\}^T, \qquad \underline{\boldsymbol{\Upsilon}} = \left\{ \begin{array}{cc} \bar{\kappa}_{122} & \bar{\kappa}_{211} \end{array} \right\}^T, \tag{46}$$

and $\underline{\underline{\mathbf{B}}}^{\Xi}$ and $\underline{\underline{\mathbf{B}}}^{\Upsilon}$ are properly derived strain localization matrices. By plugging equation (45) in equation (44), the *microscopic mean strain energy* $\bar{\mathcal{E}}^0_m$ becomes

$$\begin{aligned} \bar{\mathcal{E}}^0_m = \frac{|\mathcal{A}|}{2}\Bigg(& \underline{\boldsymbol{\Xi}}^T \int_Q \underline{\underline{\mathbf{B}}}^{\Xi T}\underline{\underline{\mathbf{C}}}^m\underline{\underline{\mathbf{B}}}^{\Xi} d\boldsymbol{\xi}\, \underline{\boldsymbol{\Xi}} + \underline{\boldsymbol{\Upsilon}}^T \int_Q \underline{\underline{\mathbf{B}}}^{\Upsilon T}\underline{\underline{\mathbf{C}}}^m\underline{\underline{\mathbf{B}}}^{\Upsilon} d\boldsymbol{\xi}\, \underline{\boldsymbol{\Upsilon}} + \\ & + \underline{\boldsymbol{\Xi}}^T \int_Q \underline{\underline{\mathbf{B}}}^{\Xi T}\underline{\underline{\mathbf{C}}}^m\underline{\underline{\mathbf{B}}}^{\Upsilon} d\boldsymbol{\xi}\, \underline{\boldsymbol{\Upsilon}} + \underline{\boldsymbol{\Upsilon}}^T \int_Q \underline{\underline{\mathbf{B}}}^{\Upsilon T}\underline{\underline{\mathbf{C}}}^m\underline{\underline{\mathbf{B}}}^{\Xi} d\boldsymbol{\xi}\, \underline{\boldsymbol{\Xi}} \Bigg). \end{aligned} \tag{47}$$

The related *microscopic mean strain energy density* is consequently derived

$$\begin{aligned} \bar{\phi}^0_m = \frac{\bar{\mathcal{E}}^0_m}{|\mathcal{A}|} = \frac{1}{2}\int_Q \underline{\boldsymbol{\varepsilon}}_0^T\underline{\underline{\mathbf{C}}}^m\underline{\boldsymbol{\varepsilon}}_0 d\boldsymbol{\xi} = \frac{1}{2}\Bigg(& \underline{\boldsymbol{\Xi}}^T \int_Q \underline{\underline{\mathbf{B}}}^{\Xi T}\underline{\underline{\mathbf{C}}}^m\underline{\underline{\mathbf{B}}}^{\Xi} d\boldsymbol{\xi}\, \underline{\boldsymbol{\Xi}} + \underline{\boldsymbol{\Upsilon}}^T \int_Q \underline{\underline{\mathbf{B}}}^{\Upsilon T}\underline{\underline{\mathbf{C}}}^m\underline{\underline{\mathbf{B}}}^{\Upsilon} d\boldsymbol{\xi}\, \underline{\boldsymbol{\Upsilon}} + \\ & + \underline{\boldsymbol{\Xi}}^T \int_Q \underline{\underline{\mathbf{B}}}^{\Xi T}\underline{\underline{\mathbf{C}}}^m\underline{\underline{\mathbf{B}}}^{\Upsilon} d\boldsymbol{\xi}\, \underline{\boldsymbol{\Upsilon}} + \underline{\boldsymbol{\Upsilon}}^T \int_Q \underline{\underline{\mathbf{B}}}^{\Upsilon T}\underline{\underline{\mathbf{C}}}^m\underline{\underline{\mathbf{B}}}^{\Xi} d\boldsymbol{\xi}\, \underline{\boldsymbol{\Xi}} \Bigg). \end{aligned} \tag{48}$$

Analogously, the macroscopic strain energy density evaluated in $\mathbf{x} = \mathbf{0}$ is introduced

$$\phi^0_M = \frac{1}{2}\left(\underline{\boldsymbol{\Gamma}}_0{}^T\underline{\underline{\mathbf{G}}}^M\underline{\boldsymbol{\Gamma}}_0 + \underline{\mathbf{K}}_0{}^T\underline{\underline{\mathbf{S}}}^M\underline{\mathbf{K}}_0 + \underline{\boldsymbol{\Gamma}}_0{}^T\underline{\underline{\mathbf{Y}}}^M\underline{\mathbf{K}}_0 + \underline{\mathbf{K}}_0{}^T\underline{\underline{\mathbf{Y}}}^{MT}\underline{\boldsymbol{\Gamma}}_0\right), \tag{49}$$

where the asymmetric micropolar strain vector and the curvature vector, evaluated evaluated in $\mathbf{x} = \mathbf{0}$, take the following form, remembering equations (40), and (41),

$$\begin{aligned} \underline{\boldsymbol{\Gamma}}_0 &= \underline{\underline{\mathbf{A}}}^{\Xi}_{\Gamma}\underline{\boldsymbol{\Xi}} + \underline{\underline{\mathbf{A}}}^{\Upsilon}_{\Gamma}\underline{\boldsymbol{\Upsilon}}, \\ \underline{\mathbf{K}}_0 &= \underline{\underline{\mathbf{A}}}^{\Xi}_{K}\underline{\boldsymbol{\Xi}} + \underline{\underline{\mathbf{A}}}^{\Upsilon}_{K}\underline{\boldsymbol{\Upsilon}}, \end{aligned} \tag{50}$$

being $\underline{\underline{\mathbf{A}}}^{\Xi}_{\Gamma}$, $\underline{\underline{\mathbf{A}}}^{\Xi}_{K}$, $\underline{\underline{\mathbf{A}}}^{\Upsilon}_{\Gamma}$, $\underline{\underline{\mathbf{A}}}^{\Upsilon}_{K}$ transformation matrices. By exploiting the generalized macro-homogeneity condition, that establishes the equivalence between the microscopic and macroscopic strain energy density $\bar{\phi}^0_m \doteq \phi^0_M$ ($\mathbf{x} = \mathbf{0}$), after some manipulations, the following relations read

$$\begin{aligned} \underline{\underline{\mathbf{A}}}^{\Xi T}_{\Gamma}\underline{\underline{\mathbf{G}}}^M\underline{\underline{\mathbf{A}}}^{\Xi}_{\Gamma} + \underline{\underline{\mathbf{A}}}^{\Xi T}_{K}\underline{\underline{\mathbf{S}}}^M\underline{\underline{\mathbf{A}}}^{\Xi}_{K} + \underline{\underline{\mathbf{A}}}^{\Xi T}_{\Gamma}\underline{\underline{\mathbf{Y}}}^M\underline{\underline{\mathbf{A}}}^{\Xi}_{K} + \underline{\underline{\mathbf{A}}}^{\Xi T}_{K}\underline{\underline{\mathbf{Y}}}^{MT}\underline{\underline{\mathbf{A}}}^{\Xi}_{\Gamma} &= \int_Q \underline{\underline{\mathbf{B}}}^{\Xi T}\underline{\underline{\mathbf{C}}}^m\underline{\underline{\mathbf{B}}}^{\Xi} d\boldsymbol{\xi}, \\ \underline{\underline{\mathbf{A}}}^{\Upsilon T}_{\Gamma}\underline{\underline{\mathbf{G}}}^M\underline{\underline{\mathbf{A}}}^{\Upsilon}_{\Gamma} + \underline{\underline{\mathbf{A}}}^{\Upsilon T}_{K}\underline{\underline{\mathbf{S}}}^M\underline{\underline{\mathbf{A}}}^{\Upsilon}_{K} + \underline{\underline{\mathbf{A}}}^{\Upsilon T}_{\Gamma}\underline{\underline{\mathbf{Y}}}^M\underline{\underline{\mathbf{A}}}^{\Upsilon}_{K} + \underline{\underline{\mathbf{A}}}^{\Upsilon T}_{K}\underline{\underline{\mathbf{Y}}}^{MT}\underline{\underline{\mathbf{A}}}^{\Upsilon}_{\Gamma} &= \int_Q \underline{\underline{\mathbf{B}}}^{\Upsilon T}\underline{\underline{\mathbf{C}}}^m\underline{\underline{\mathbf{B}}}^{\Upsilon} d\boldsymbol{\xi}, \\ \underline{\underline{\mathbf{A}}}^{\Upsilon T}_{\Gamma}\underline{\underline{\mathbf{G}}}^M\underline{\underline{\mathbf{A}}}^{\Xi}_{\Gamma} + \underline{\underline{\mathbf{A}}}^{\Upsilon T}_{K}\underline{\underline{\mathbf{S}}}^M\underline{\underline{\mathbf{A}}}^{\Xi}_{K} + \underline{\underline{\mathbf{A}}}^{\Upsilon T}_{\Gamma}\underline{\underline{\mathbf{Y}}}^M\underline{\underline{\mathbf{A}}}^{\Xi}_{K} + \underline{\underline{\mathbf{A}}}^{\Upsilon T}_{K}\underline{\underline{\mathbf{Y}}}^{MT}\underline{\underline{\mathbf{A}}}^{\Xi}_{\Gamma} &= \int_Q \underline{\underline{\mathbf{B}}}^{\Upsilon T}\underline{\underline{\mathbf{C}}}^m\underline{\underline{\mathbf{B}}}^{\Xi} d\boldsymbol{\xi}, \\ \underline{\underline{\mathbf{A}}}^{\Xi T}_{\Gamma}\underline{\underline{\mathbf{G}}}^M\underline{\underline{\mathbf{A}}}^{\Upsilon}_{\Gamma} + \underline{\underline{\mathbf{A}}}^{\Xi T}_{K}\underline{\underline{\mathbf{S}}}^M\underline{\underline{\mathbf{A}}}^{\Upsilon}_{K} + \underline{\underline{\mathbf{A}}}^{\Xi T}_{\Gamma}\underline{\underline{\mathbf{Y}}}^M\underline{\underline{\mathbf{A}}}^{\Upsilon}_{K} + \underline{\underline{\mathbf{A}}}^{\Xi T}_{K}\underline{\underline{\mathbf{Y}}}^{MT}\underline{\underline{\mathbf{A}}}^{\Upsilon}_{\Gamma} &= \int_Q \underline{\underline{\mathbf{B}}}^{\Xi T}\underline{\underline{\mathbf{C}}}^m\underline{\underline{\mathbf{B}}}^{\Upsilon} d\boldsymbol{\xi}. \end{aligned} \tag{51}$$

It follows that the overall elastic micropolar matrices, in symmetrized forms, can be, thus, obtained by solving the set of equations (51) and result as

$$
\begin{aligned}
\underline{\underline{\mathbf{G}}}^{M} &= \int_{Q} \underline{\underline{\mathbf{L}}}_{\Gamma}^{\Xi-T} \underline{\underline{\mathbf{F}}}^{\Xi T} \underline{\underline{\mathbf{C}}}^{m} \underline{\underline{\mathbf{F}}}^{\Xi} \underline{\underline{\mathbf{L}}}_{\Gamma}^{\Xi-1} d\boldsymbol{\xi} - \int_{Q} \underline{\underline{\mathbf{L}}}_{\Gamma}^{\Xi-T} \underline{\underline{\mathbf{A}}}_{\Gamma}^{\Xi T} \underline{\underline{\mathbf{L}}}_{\Gamma}^{\Xi-T} \underline{\underline{\mathbf{F}}}^{\Xi T} \underline{\underline{\mathbf{C}}}^{m} \underline{\underline{\mathbf{F}}}^{\Upsilon} \underline{\underline{\mathbf{L}}}_{K}^{\Upsilon-1} \underline{\underline{\mathbf{A}}}_{K}^{\Xi} \underline{\underline{\mathbf{L}}}_{\Gamma}^{\Xi-1} d\boldsymbol{\xi} + \\
&- \int_{Q} \underline{\underline{\mathbf{L}}}_{\Gamma}^{\Xi-T} \underline{\underline{\mathbf{A}}}_{K}^{\Xi T} \underline{\underline{\mathbf{L}}}_{K}^{\Upsilon-T} \underline{\underline{\mathbf{F}}}^{\Upsilon T} \underline{\underline{\mathbf{C}}}^{m} \underline{\underline{\mathbf{F}}}^{\Xi} \underline{\underline{\mathbf{L}}}_{\Gamma}^{\Xi-1} \underline{\underline{\mathbf{A}}}_{\Gamma}^{\Xi} \underline{\underline{\mathbf{L}}}_{\Gamma}^{\Xi-1} d\boldsymbol{\xi} + \\
&+ \int_{Q} \underline{\underline{\mathbf{L}}}_{\Gamma}^{\Xi-T} \underline{\underline{\mathbf{A}}}_{K}^{\Xi T} \underline{\underline{\mathbf{A}}}_{K}^{\Upsilon-T} \underline{\underline{\mathbf{A}}}_{\Gamma}^{\Upsilon T} \underline{\underline{\mathbf{L}}}_{\Gamma}^{\Xi-T} \underline{\underline{\mathbf{F}}}^{\Xi T} \underline{\underline{\mathbf{C}}}^{m} \underline{\underline{\mathbf{F}}}^{\Upsilon} \underline{\underline{\mathbf{L}}}_{K}^{\Upsilon-1} \underline{\underline{\mathbf{A}}}_{K}^{\Xi} \underline{\underline{\mathbf{L}}}_{\Gamma}^{\Xi-1} d\boldsymbol{\xi} + \\
&+ \int_{Q} \underline{\underline{\mathbf{L}}}_{\Gamma}^{\Xi-T} \underline{\underline{\mathbf{A}}}_{K}^{\Xi T} \underline{\underline{\mathbf{L}}}_{K}^{\Upsilon-T} \underline{\underline{\mathbf{F}}}^{\Upsilon T} \underline{\underline{\mathbf{C}}}^{m} \underline{\underline{\mathbf{F}}}^{\Xi} \underline{\underline{\mathbf{L}}}_{\Gamma}^{\Xi-1} \underline{\underline{\mathbf{A}}}_{\Gamma}^{\Upsilon} \underline{\underline{\mathbf{A}}}_{K}^{\Upsilon-1} \underline{\underline{\mathbf{A}}}_{K}^{\Xi} \underline{\underline{\mathbf{L}}}_{\Gamma}^{\Xi-1} d\boldsymbol{\xi}, \\
\underline{\underline{\mathbf{S}}}^{M} &= \int_{Q} \underline{\underline{\mathbf{L}}}_{K}^{\Upsilon-T} \underline{\underline{\mathbf{F}}}^{\Upsilon T} \underline{\underline{\mathbf{C}}}^{m} \underline{\underline{\mathbf{F}}}^{\Upsilon} \underline{\underline{\mathbf{L}}}_{K}^{\Upsilon-1} d\boldsymbol{\xi} - \int_{Q} \underline{\underline{\mathbf{L}}}_{K}^{\Upsilon-T} \underline{\underline{\mathbf{A}}}_{\Gamma}^{\Upsilon T} \underline{\underline{\mathbf{L}}}_{\Gamma}^{\Xi-T} \underline{\underline{\mathbf{F}}}^{\Xi T} \underline{\underline{\mathbf{C}}}^{m} \underline{\underline{\mathbf{F}}}^{\Upsilon} \underline{\underline{\mathbf{L}}}_{K}^{\Upsilon-1} \underline{\underline{\mathbf{A}}}_{K}^{\Upsilon} \underline{\underline{\mathbf{L}}}_{K}^{\Upsilon-1} d\boldsymbol{\xi} + \\
&- \int_{Q} \underline{\underline{\mathbf{L}}}_{K}^{\Upsilon-T} \underline{\underline{\mathbf{A}}}_{K}^{\Upsilon T} \underline{\underline{\mathbf{L}}}_{K}^{\Upsilon-T} \underline{\underline{\mathbf{F}}}^{\Upsilon T} \underline{\underline{\mathbf{C}}}^{m} \underline{\underline{\mathbf{F}}}^{\Xi} \underline{\underline{\mathbf{L}}}_{\Gamma}^{\Xi-1} \underline{\underline{\mathbf{A}}}_{\Gamma}^{\Upsilon} \underline{\underline{\mathbf{L}}}_{K}^{\Upsilon-1} d\boldsymbol{\xi} + \\
&+ \int_{Q} \underline{\underline{\mathbf{L}}}_{K}^{\Upsilon-T} \underline{\underline{\mathbf{A}}}_{\Gamma}^{\Upsilon T} \underline{\underline{\mathbf{A}}}_{\Gamma}^{\Xi-T} \underline{\underline{\mathbf{A}}}_{K}^{\Xi T} \underline{\underline{\mathbf{L}}}_{K}^{\Upsilon-T} \underline{\underline{\mathbf{F}}}^{\Upsilon T} \underline{\underline{\mathbf{C}}}^{m} \underline{\underline{\mathbf{F}}}^{\Xi} \underline{\underline{\mathbf{L}}}_{\Gamma}^{\Xi-1} \underline{\underline{\mathbf{A}}}_{\Gamma}^{\Upsilon} \underline{\underline{\mathbf{L}}}_{K}^{\Upsilon-1} d\boldsymbol{\xi} + \\
&+ \int_{Q} \underline{\underline{\mathbf{L}}}_{K}^{\Upsilon-T} \underline{\underline{\mathbf{A}}}_{\Gamma}^{\Upsilon T} \underline{\underline{\mathbf{L}}}_{\Gamma}^{\Xi-T} \underline{\underline{\mathbf{F}}}^{\Xi T} \underline{\underline{\mathbf{C}}}^{m} \underline{\underline{\mathbf{F}}}^{\Upsilon} \underline{\underline{\mathbf{L}}}_{K}^{\Upsilon-1} \underline{\underline{\mathbf{A}}}_{K}^{\Xi} \underline{\underline{\mathbf{A}}}_{\Gamma}^{\Xi-1} \underline{\underline{\mathbf{A}}}_{\Gamma}^{\Upsilon} \underline{\underline{\mathbf{L}}}_{K}^{\Upsilon-1} d\boldsymbol{\xi}, \\
\underline{\underline{\mathbf{Y}}}^{M} &= \int_{Q} \underline{\underline{\mathbf{L}}}_{\Gamma}^{\Xi-T} \underline{\underline{\mathbf{F}}}^{\Xi T} \underline{\underline{\mathbf{C}}}^{m} \underline{\underline{\mathbf{F}}}^{\Upsilon} \underline{\underline{\mathbf{L}}}_{K}^{\Upsilon-1} d\boldsymbol{\xi},
\end{aligned}
\tag{52}
$$

with the auxiliary matrices $\underline{\underline{\mathbf{F}}}^{\Xi}$ and $\underline{\underline{\mathbf{F}}}^{\Upsilon}$ depending on both the localization and the transformation matrices, that is

$$
\begin{aligned}
\underline{\underline{\mathbf{F}}}^{\Xi} &= \underline{\underline{\mathbf{B}}}^{\Xi} - \underline{\underline{\mathbf{B}}}^{\Upsilon} \underline{\underline{\mathbf{A}}}_{K}^{\Upsilon-1} \underline{\underline{\mathbf{A}}}_{K}^{\Xi}, \\
\underline{\underline{\mathbf{F}}}^{\Upsilon} &= \underline{\underline{\mathbf{B}}}^{\Upsilon} - \underline{\underline{\mathbf{B}}}^{\Xi} \underline{\underline{\mathbf{A}}}_{\Gamma}^{\Xi-1} \underline{\underline{\mathbf{A}}}_{\Gamma}^{\Upsilon},
\end{aligned}
\tag{53}
$$

and the matrices $\underline{\underline{\mathbf{L}}}_{\Gamma}^{\Xi}$ and $\underline{\underline{\mathbf{L}}}_{K}^{\Upsilon}$ take the following form in terms of the transformation matrices

$$
\begin{aligned}
\underline{\underline{\mathbf{L}}}_{\Gamma}^{\Xi} &= \underline{\underline{\mathbf{A}}}_{\Gamma}^{\Xi} - \underline{\underline{\mathbf{A}}}_{\Gamma}^{\Upsilon} \underline{\underline{\mathbf{A}}}_{K}^{\Upsilon-1} \underline{\underline{\mathbf{A}}}_{K}^{\Xi}, \\
\underline{\underline{\mathbf{L}}}_{K}^{\Upsilon} &= \underline{\underline{\mathbf{A}}}_{K}^{\Upsilon} - \underline{\underline{\mathbf{A}}}_{K}^{\Xi} \underline{\underline{\mathbf{A}}}_{\Gamma}^{\Xi-1} \underline{\underline{\mathbf{A}}}_{\Gamma}^{\Upsilon}.
\end{aligned}
\tag{54}
$$

In the case the periodic cell is characterized by centrosymmetric topology, the relations $\underline{\underline{\mathbf{F}}}^{\Xi} = \underline{\underline{\mathbf{B}}}^{\Xi}$, $\underline{\underline{\mathbf{F}}}^{\Upsilon} = \underline{\underline{\mathbf{B}}}^{\Upsilon}$, $\underline{\underline{\mathbf{L}}}_{\Gamma}^{\Xi} = \underline{\underline{\mathbf{A}}}_{\Gamma}^{\Xi}$, $\underline{\underline{\mathbf{L}}}_{K}^{\Upsilon} = \underline{\underline{\mathbf{A}}}_{K}^{\Upsilon}$ hold, thus the overall elastic micropolar matrices specialize in

$$
\begin{aligned}
\underline{\underline{\mathbf{G}}}^{M} &= \int_{Q} \underline{\underline{\mathbf{A}}}_{\Gamma}^{\Xi-T} \underline{\underline{\mathbf{B}}}^{\Xi T} \underline{\underline{\mathbf{C}}}^{m} \underline{\underline{\mathbf{B}}}^{\Xi} \underline{\underline{\mathbf{A}}}_{\Gamma}^{\Xi-1} d\boldsymbol{\xi}, \\
\underline{\underline{\mathbf{S}}}^{M} &= \int_{Q} \underline{\underline{\mathbf{A}}}_{K}^{\Upsilon-T} \underline{\underline{\mathbf{B}}}^{\Upsilon T} \underline{\underline{\mathbf{C}}}^{m} \underline{\underline{\mathbf{B}}}^{\Upsilon} \underline{\underline{\mathbf{A}}}_{K}^{\Upsilon-1} d\boldsymbol{\xi},
\end{aligned}
\tag{55}
$$

and the coupling matrix is $\underline{\underline{\mathbf{Y}}}^{M} = \mathbf{0}$. It is worth noting that, in the extreme case of homogeneous material at the microscopic scale, i.e. vanishing mismatch between elastic moduli of constituents in the periodic

cell, also the nonlocal elastic matrix is $\underline{\underline{\mathbf{S}}}^{M} = \mathbf{0}$, since the perturbation functions are identically zero.
An alternative way to determine the overall elastic matrices of the equivalent micropolar continuum $\underline{\underline{\mathbf{G}}}^{M}$, $\underline{\underline{\mathbf{S}}}^{M}$, and $\underline{\underline{\mathbf{Y}}}^{M}$, collected in the block matrix $\underline{\underline{\mathbf{C}}}^{M(mp)}$ (see Appendix B, equation (B.6)), can be obtained considering the vector $\underline{\mathbf{\Psi}}$ in terms of the two vectors $\underline{\Xi}$ and $\underline{\Upsilon}$, that is

$$\underline{\mathbf{\Psi}} = \left\{ \begin{array}{cc} \underline{\Xi} & \underline{\Upsilon} \end{array} \right\}^{T}, \tag{56}$$

and, thus, expressing the strain vector $\boldsymbol{\varepsilon}_0$, as a variant of equation (45), i.e.

$$\underline{\boldsymbol{\varepsilon}}_0 = \underline{\underline{\mathbf{B}}}^{(\Xi,\Upsilon)} \underline{\mathbf{\Psi}}, \tag{57}$$

where the localization block matrix $\underline{\underline{\mathbf{B}}}^{(\Xi,\Upsilon)}$ has been introduced. Therefore, the *microscopic mean strain energy density* becomes

$$\bar{\phi}^{0}_{m} = \frac{1}{2} \underline{\mathbf{\Psi}}^{T} \int_{Q} \underline{\underline{\mathbf{B}}}^{(\Xi,\Upsilon)^{T}} \underline{\underline{\mathbf{C}}}^{m} \underline{\underline{\mathbf{B}}}^{(\Xi,\Upsilon)} d\boldsymbol{\xi} \, \underline{\mathbf{\Psi}}. \tag{58}$$

Moreover, the macroscopic strain energy density can be alternatively expressed as

$$\phi^{0}_{M} = \frac{1}{2} \left(\underline{\mathbf{E}}^{(mp)^{T}}_{0} \underline{\underline{\mathbf{C}}}^{M(mp)} \underline{\mathbf{E}}^{(mp)}_{0} \right), \tag{59}$$

where

$$\underline{\mathbf{E}}^{(mp)}_{0} = \underline{\underline{\mathbf{A}}}^{(\Xi,\Upsilon)} \underline{\mathbf{\Psi}}. \tag{60}$$

being $\underline{\underline{\mathbf{A}}}^{(\Xi,\Upsilon)}$ the block transformation matrix. By exploiting the macro-homogeneity condition, the final form of the overall elastic block matrix reads

$$\underline{\underline{\mathbf{C}}}^{M(mp)} = \underline{\underline{\mathbf{A}}}^{(\Xi,\Upsilon)^{-T}} \int_{Q} \underline{\underline{\mathbf{B}}}^{(\Xi,\Upsilon)^{T}} \underline{\underline{\mathbf{C}}}^{M(mp)} \underline{\underline{\mathbf{B}}}^{(\Xi,\Upsilon)} d\boldsymbol{\xi} \, \underline{\underline{\mathbf{A}}}^{(\Xi,\Upsilon)^{-1}}. \tag{61}$$

4. Illustrative applications: homogenization of a bi-phase material

In this section, some illustrative examples of technological interest are proposed to assess the capabilities of the proposed homogenization technique. In Subsection 4.1, the periodic perturbation functions characterizing a two-phase composite material with cubic symmetry and isolated inclusions are determined as solution of the nested cell problems. The related micropolar homogenized elastic tensors are consistently derived. In this context, a parametric analysis is performed in order to deduce the influence of the microstructural mechanical properties on the overall constitutive ones. Subsections 4.2 and 4.3 are, finally, devoted to the solution of two benchmark problems. In the former, the analytical results obtained as solution of the homogenized model are compared with a micro-mechanical finite element analysis. In the latter, instead, a complex loading condition is applied on an infinite strip. The results are critically commented. Finite Element analyses have been performed to solve the numerical problems at both macroscopic and microscopic scale.

4.1. Perturbation functions solution of hierarchical PDE Cell Problems and micropolar equivalent constants

A two-phase periodic medium, made of square inclusions regularly distributed within a base matrix, is considered. The related square periodic cell, having size ε=1 mm, is shown in Figure 3. Both constituents are assumed isotropic, perfectly bonded and in plane strain conditions. In the following, the ratios between the Young's moduli and the Poisson ratios of inclusion and matrix are denoted by $\eta_E = E_2/E_1$,

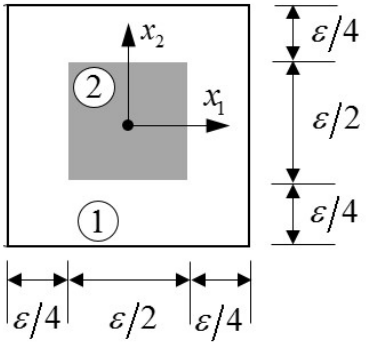

Figure 3: Schematic of the periodic cell $\mathcal{A}$.

and $\eta_\nu = \nu_2/\nu_1$, respectively.
First, the *cell problems*, equations (11)–(16) at the orders ε^{-1}, ε^0 and ε^1, respectively, are numerically solved in order to derive the perturbation functions $N^{(l)}_{ijq}$ for a unit cell Q characterized by $E_2 = 0.5$ GPa and $E_1 = 500$ GPa, i.e. ratios $\eta_E = 10^{-3}$, and $\eta_\nu = 1$, with $\nu_2 = \nu_1 = 0.1$. In Figures 4, 5, and 6, selected contour plots of perturbation functions, $N^{(1)}_{ijq_1}$, $N^{(2)}_{ijq_1q_2}$, and $N^{(3)}_{ijq_1q_2q_3}$ are reported, respectively. It emerges that the perturbation functions are Q-periodic, smooth along the cell boundaries, and characterized by zero mean values within Q according to the *normalization conditions*. By exploiting the perturbation functions and determining the macroscopic elastic tensor of the first order homogeneous continuum via equation (25), the overall constitutive tensors of the micropolar homogenized medium are, then, computed. It is observed that, due the centro-symmetric microstructure, the coupling overall constitutive matrix $\underline{\underline{\mathbf{Y}}}^M$ is identically zero. Thus, the non-vanishing overall elastic matrices are the following

$$\underline{\underline{\mathbf{G}}}^M = \begin{bmatrix} 27.469 & 2.5347 & 0 & 0 \\ 2.5347 & 27.469 & 0 & 0 \\ 0 & 0 & 12.896 & -2.3544 \\ 0 & 0 & -2.3544 & 12.9369 \end{bmatrix} 10^4 \text{ MPa},$$

$$\underline{\underline{\mathbf{S}}}^M = \begin{bmatrix} 1.1769 & 0 \\ 0 & 1.1769 \end{bmatrix} 10^3 \text{ MPa mm}^2.$$

The same analyses have been repeated considering a first case where η_E varies, by fixing E_1=500 GPa, and ν_1=ν_2=0.1, and a second case in which, instead, η_ν varies by fixing ν_1=0.1 and E_1=E_2=500 GPa. The results of this parametric analysis are obtained by exploiting the micropolar constitutive equations for the general case in the following component form

$$\begin{aligned} \Sigma_{(ij)} &= G_{(ij)(hk)}\Gamma_{(hk)} + G_{(ij)[hk]}\Gamma_{[hk]} + Y_{(ij)h}\mathrm{K}_h, \\ \Sigma_{[ij]} &= G_{[ij](hk)}\Gamma_{(hk)} + G_{[ij][hk]}\Gamma_{[hk]} + Y_{[ij]h}\mathrm{K}_h, \\ \mathrm{M}_h &= Y_{(ij)h}\Gamma_{(ij)} + Y_{[ij]h}\Gamma_{[ij]} + S_{hk}\mathrm{K}_k, \end{aligned} \tag{62}$$

where the split between the symmetric and skew-symmetric components of the tensors $\mathbf{\Sigma}$, and $\mathbf{\Gamma}$ is performed, i.e. $\Sigma_{(ij)} = \frac{1}{2}\left(\Sigma_{ij} + \Sigma_{ji}\right)$, $\Sigma_{[ij]} = \frac{1}{2}\left(\Sigma_{ij} - \Sigma_{ji}\right)$, $\Gamma_{(ij)} = \frac{1}{2}\left(\Gamma_{ij} + \Gamma_{ji}\right)$, $\Gamma_{[ij]} = \frac{1}{2}\left(\Gamma_{ij} - \Gamma_{ji}\right)$, and the

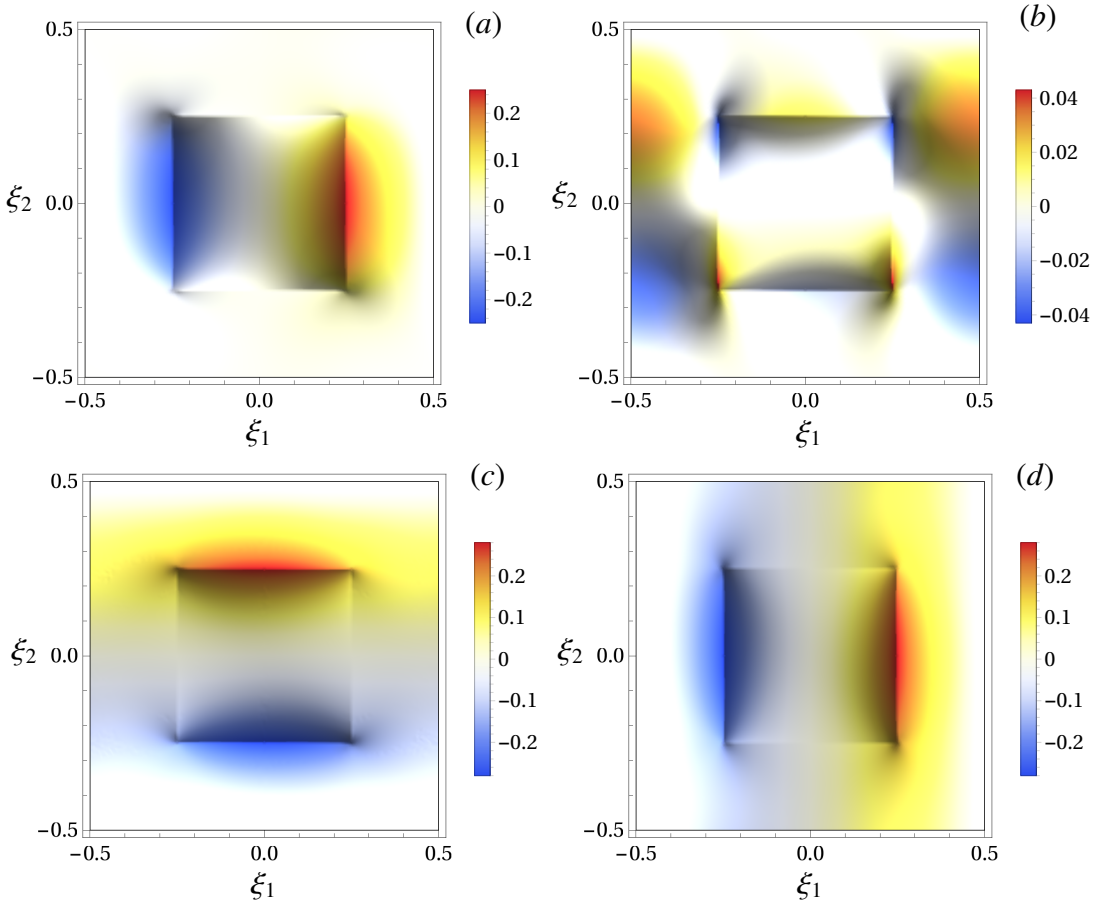

Figure 4: Contour plots of perturbation functions: (a) $N^{(1)}_{111}$; (b) $N^{(1)}_{211}$; (c) $N^{(1)}_{112}$; (d) $N^{(1)}_{212}$.

associated constitutive components are

$$
\begin{aligned}
G_{(ij)(hk)} &= \frac{1}{4}\left(G_{ijhk} + G_{ijkh} + G_{jihk} + G_{jikh}\right),\\
G_{[ij][hk]} &= \frac{1}{4}\left(G_{ijhk} - G_{ijkh} - G_{jihk} + G_{jikh}\right),\\
G_{(ij)[hk]} &= G_{[hk](ij)} = \frac{1}{4}\left(G_{ijhk} - G_{ijkh} + G_{jihk} - G_{jikh}\right),\\
Y_{(ij)h} &= \frac{1}{2}\left(Y_{ijh} + Y_{jih}\right),\\
Y_{[ij]h} &= \frac{1}{2}\left(Y_{ijh} - Y_{jih}\right).
\end{aligned}
\tag{63}
$$

In Figure 7(a), the dimensionless components $G_{(ij)(hk)}/E_1$ of the overall elasticity matrix $\underline{\underline{\mathbf{G}}}^M$, with E_1 being the Young modulus of the matrix, are plotted against $\eta_E \in [3/50, 10^3]$ in a semi-log plot. The blue, red and green curves correspond to the components $G_{1111} = G_{2222}$, G_{1122}, $G_{(12)(12)}$, respectively. In particular, a monotonic increasing trend is observed, as the Young modulus of the inclusions increases, i.e. ranging from inclusions softer or stiffer than the matrix. Figure 7(b) shows the dimensionless components $G_{[ij][hk]}/E_1$ versus η_E in a semi-log plot. In this case it is worth noting that a singularity occurs at $\eta_E = 1$, that is when, as the microstructure vanishes, a Cauchy homogeneous material is considered. This circumstance is due to the fact that the skew-symmetric components of the strain tensor $\boldsymbol{\Gamma}$ is not defined for a Cauchy homogeneous continuum. Finally, in Figure 7(c) the characteristic lengths λ_1/ε, and $\widetilde{\lambda}_1/\varepsilon$ (see equation (69)) are reported, in a semi-log plot against η_E. As expected at η_E=1, i.e. in the limit case of locally homogeneous material, both the characteristic lengths vanish, since the nonlocal constitutive matrix $\underline{\underline{\mathbf{S}}}^M$ vanishes in turn, recovering a well known feature of the classical Cauchy medium.

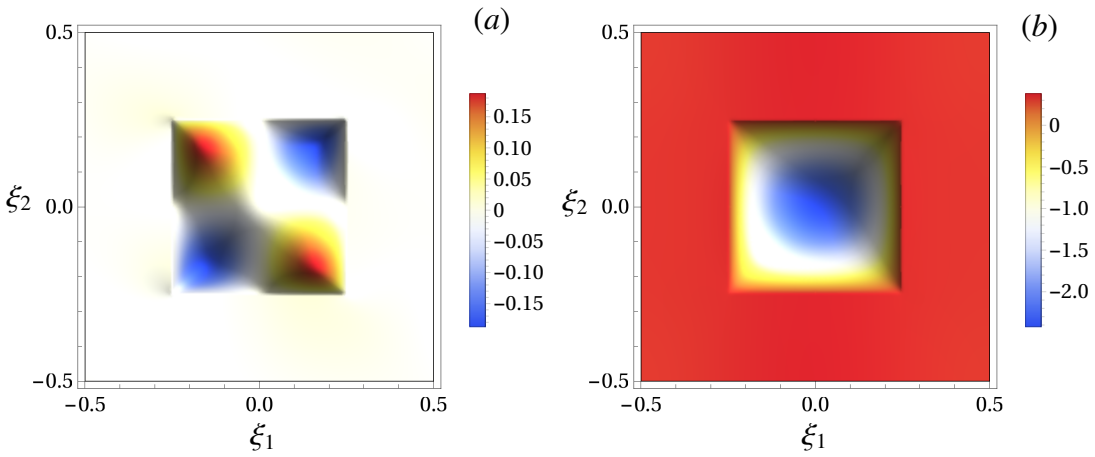

Figure 5: Contour plots of perturbation functions: (a) $N^{(2)}_{1211}$; (b) $N^{(2)}_{2211}$.

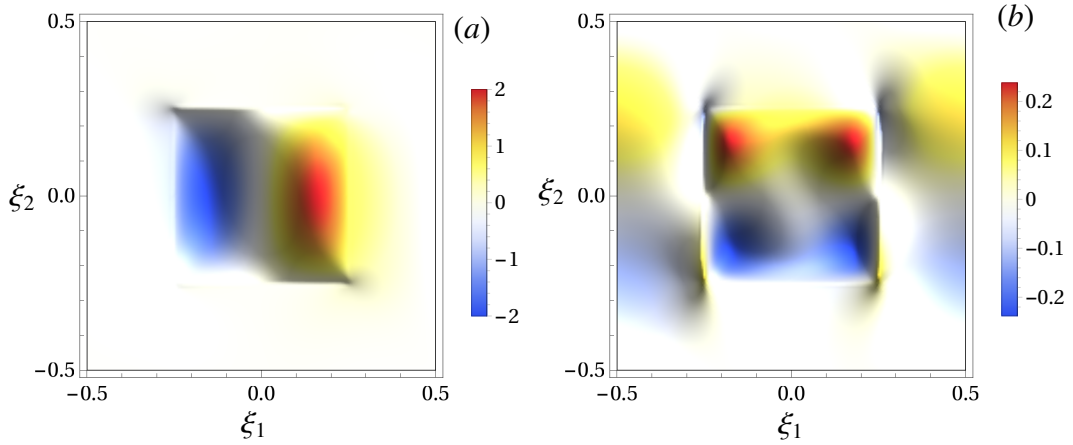

Figure 6: Contour plots of perturbation functions: (a) $N^{(3)}_{11111}$; (b) $N^{(3)}_{21111}$.

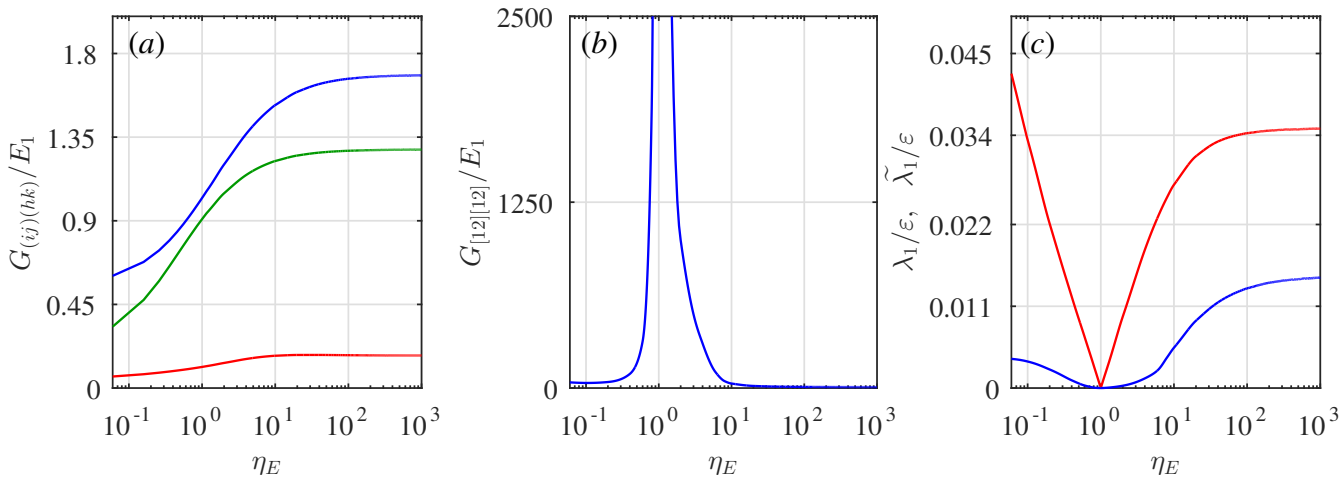

Figure 7: Micropolar equivalent material: classical and micropolar homogenized elastic coefficients versus $\eta_E = E_2/E_1$ versus $\eta_E \in [3/50, 10^3]$. (a) blue curve $G_{1111} = G_{2222}$; red curve G_{1122}; green curve $G_{(12)(12)}$; (b) component $G_{[12][12]}$; (c) characteristic lengths λ_1/ε, and $\widetilde{\lambda}_1/\varepsilon$.

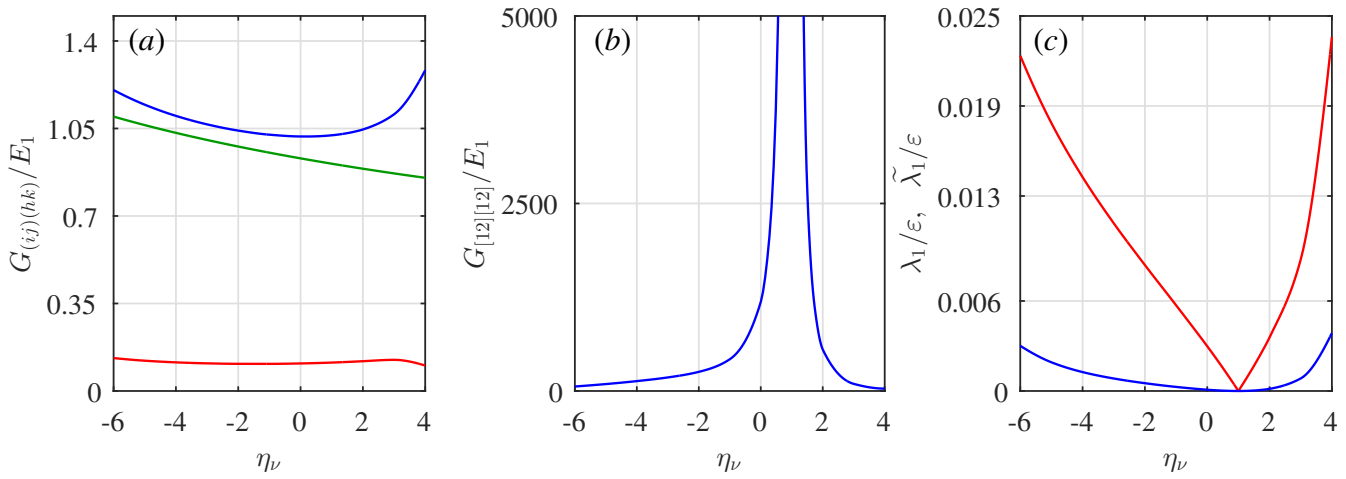

Figure 8: Micropolar equivalent material: classical and micropolar homogenized elastic coefficients versus $\eta_E = E_2/E_1$ versus η_{nu}. (a) blue curve $G_{1111} = G_{2222}$; red curve G_{1122}; green curve $G_{(12)(12)}$; (b) component $G_{[12][12]}$; (c) characteristic lengths λ_1/ε, and $\widetilde{\lambda}_1/\varepsilon$.

Analogously, in Figure 8, the dimensionless components $G_{(ij)(hk)}/E_1$, $G_{[ij][hk]}/E_1$, and the characteristic lengths λ_1/ε, and $\widetilde{\lambda}_1/\varepsilon$ are reported against η_ν. In Figure 8(a), considerably smaller variations of the components $G_{(ij)(hk)}/E_1$, compared to the respective Figure 7(a), are found. Moreover, it emerges that for η_ν=1, i.e. Cauchy homogeneous material, both a singularity is found in Figure 8(b), and a zero value point is shown in Figure 8(c).

4.2. Benchmark 1: Infinite periodic medium undergoing harmonic body forces

An infinite two-phase periodic medium is considered (see Figure 9) undergoing $\mathcal{L}$-periodic harmonic

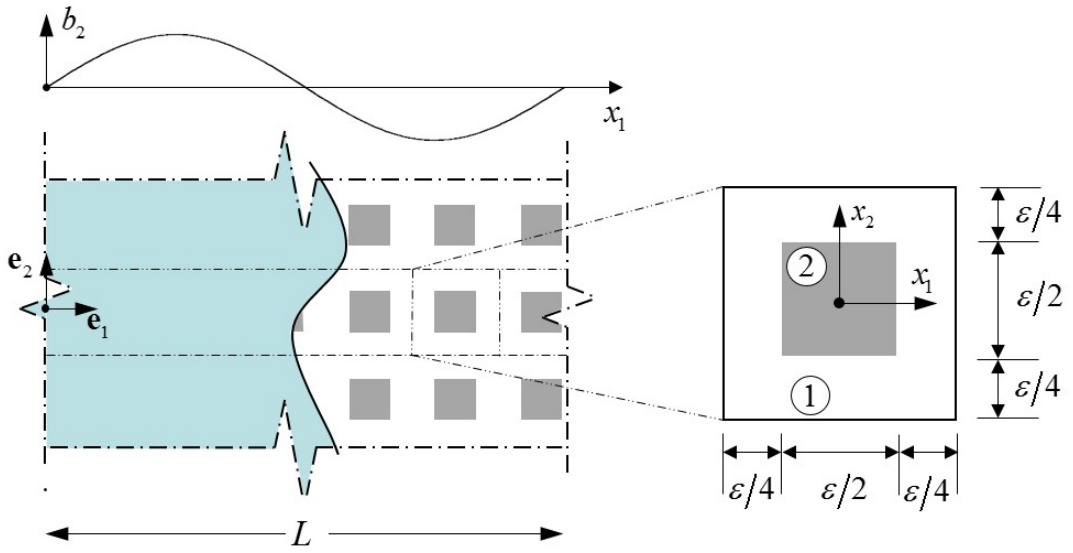

Figure 9: Schematic of the heterogeneous medium versus the respective homogenized one (in light blue) undergoing harmonic body forces $b_2(x_1)$, and a zoom on the two-phase periodic cell having size ε.

body forces with non vanishing component

$$b_2(x_1) = \imath \Xi_2 e^{\imath\left(2\pi n \frac{x_1}{L_1}\right)}, \tag{64}$$

being $n \in \mathbb{Z}^*$ the wave number, $\imath^2 = -1$ the imaginary unit, Ξ_2 the amplitude of $b_2(x_1)$ and L_1 the wave length coinciding with the structural length L. Plane strain conditions are assumed. By exploiting the

periodicity of both heterogeneous material and volume forces, it is possible to restrict the problem to a limited portion of the heterogeneous medium, as schematically shown in Figure 9. Moreover, since the body forces are invariant with respect to x_2, a cluster of L/ε periodic cells along direction $\mathbf{e}_1$ can be considered.
The macroscopic micropolar governing equations (6), thus, specialize into

$$\begin{aligned} &G_{1221}\frac{\partial \Phi}{\partial x_1} + G_{2121}\left(\frac{\partial^2 U_2}{\partial {x_1}^2} - \frac{\partial \Phi}{\partial x_1}\right) + b_2 = 0, \\ &S_{11}\frac{\partial^2 \Phi}{\partial {x_1}^2} + (G_{2121} - G_{1221})\frac{\partial U_2}{\partial x_1} + (2G_{1221} - G_{1212} - G_{2121})\,\Phi = 0, \end{aligned} \tag{65}$$

and after some manipulations they result as

$$\begin{aligned} &\frac{\partial^3 \Phi}{\partial {x_1}^3} - \frac{G_{2121}G_{1212} - {G_{1221}}^2}{S_{11}G_{2121}}\frac{\partial \Phi}{\partial x_1} - \frac{G_{2121} - G_{1221}}{S_{11}G_{2121}}b_2 = 0, \\ &\frac{\partial U_2}{\partial x_1} + \frac{S_{11}}{G_{2121} - G_{1221}}\frac{\partial^2 \Phi}{\partial {x_1}^2} - \frac{2G_{1221} - G_{1212} - G_{2121}}{G_{2121} - G_{1221}}\Phi = 0. \end{aligned} \tag{66}$$

The analytic solution of equations (66) is found in terms of $\Phi(x_1)$ and $U_2(x_1)$, and takes the form

$$\begin{aligned} &\Phi(x_1) = Ae^{\imath\left(2\pi n\frac{x_1}{L_1}\right)}, \\ &U_2(x_1) = \imath Be^{\imath\left(2\pi n\frac{x_1}{L_1}\right)}, \end{aligned} \tag{67}$$

where the coefficients A and B result

$$\begin{aligned} A &= -\frac{\frac{G_{2121}-G_{1221}}{S_{11}G_{2121}}\Xi_2}{\left(\frac{2\pi n}{L_1}\right)^3 + \frac{2\pi n}{L_1}\left(\frac{1}{\lambda_1}\right)^2}, \\ B &= -A\frac{L}{2\pi n}\left(\left(2\pi n\frac{\tilde{\lambda}_1}{L_1}\right)^2 - \psi_1\right), \end{aligned} \tag{68}$$

with characteristic lengths λ_1, $\widetilde{\lambda_1}$ and the coefficient ψ_1 expressed in the following form

$$\begin{aligned} \lambda_1 &= \sqrt{\frac{S_{11}G_{2121}}{G_{2121}G_{1212} - {G_{1221}}^2}}, \\ \tilde{\lambda}_1 &= \sqrt{\frac{S_{11}}{G_{2121} - G_{1221}}}, \\ \psi_1 &= \frac{2G_{1221} - G_{1212} - G_{2121}}{G_{2121} - G_{1221}}. \end{aligned} \tag{69}$$

In the case $b_2(x_1) = -\Xi_2 \sin\left(2\pi n\frac{x_1}{L_1}\right)$, the solution becomes

$$\begin{aligned} \Phi(x_1) &= \frac{\frac{G_{1221}-G_{2121}}{S_{11}G_{2121}}\Xi_2}{\left(\frac{2\pi n}{L_1}\right)^3 + \frac{2\pi n}{L_1}\left(\frac{1}{\lambda_1}\right)^2}\cos\left(2\pi n\frac{x_1}{L_1}\right), \\ U_2(x_1) &= \frac{\frac{L_1}{2\pi n}\left(\left(2\pi n\frac{\tilde{\lambda}_1}{L_1}\right)^2 - \psi_1\right)\frac{G_{1221}-G_{2121}}{S_{11}G_{2121}}\Xi_2}{\left(\frac{2\pi n}{L_1}\right)^3 + \frac{2\pi n}{L}\left(\frac{1}{\lambda_1}\right)^2}\sin\left(2\pi n\frac{x_1}{L_1}\right), \end{aligned} \tag{70}$$

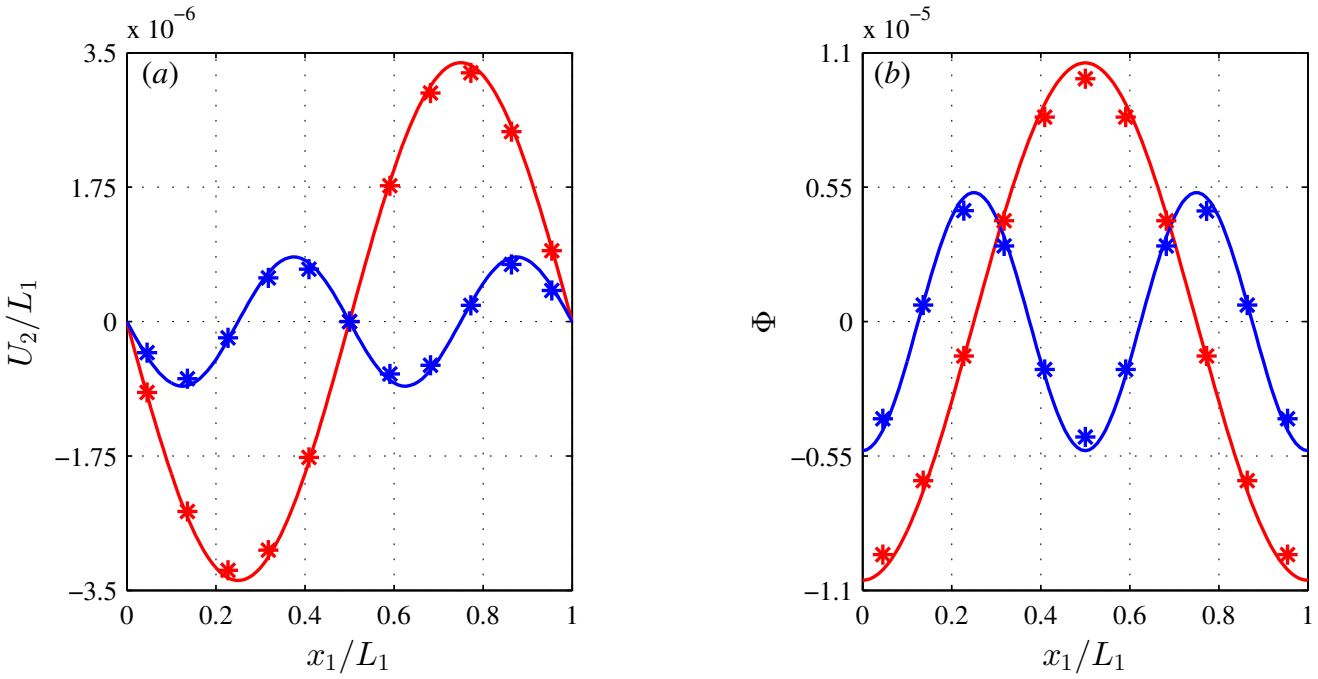

Figure 10: Case with stiffer inclusion, $\eta_E = 10^3$, η_ν=1. Comparison between macroscopic analytical solutions (solid lines) and macroscopic fields obtained from micro-mechanical results via upscaling relations (stars). Red and blue solid lines and stars refer to harmonic body forces characterized by wave number n=1, n=2, respectively. (a) U_2/L_1 vs x_1/L_1; (b) Φ vs x_1/L_1.

where the equations (70) are equivalent to the real part of (67). The macroscopic analytical solution and (70), in terms of macrodisplacement and micropolar rotation field, is compared with the micromechanical finite element solution obtained considering a portion (cluster of L/ε periodic cells along direction $\mathbf{e}_1$) of the heterogeneous material with proper periodic boundary conditions. In particular, the micromechanical displacement fields are integrated by exploiting the upscaling relations (26), (39) in order to determine the corresponding macroscopic fields.

Two different heterogeneous materials are analyzed, characterized by the same matrix (E_1= 500 GPa, ν_1=0.1) and either a softer or a stiffer inclusion, with $\eta_E = 3/50$, $\eta_\nu = 1$, and $\eta_E = 10^3$, $\eta_\nu = 1$, respectively. In both cases L/ε=11 along direction $\mathbf{e}_1$ is considered. In Figure 10, the case with $\eta_E = 10^3$, $\eta_\nu = 1$ is investigated. The analytic solutions, reported in solid lines, are compared with the respective values (plotted as stars), obtained, via upscaling relations, from the numerical results of the heterogeneous model. Red and blue solid lines and stars refer to harmonic body forces characterized by wave number n=1, n=2, respectively. In particular, in Figures 10(a) and 10(b), the dimensionless macrodisplacement U_2/L_1 and the micropolar rotation Φ are plotted versus the dimensionless macroscopic coordinate x_1/L_1, respectively. A good agreement between analytic macroscopic and numerical micromechanical solutions is found for both U_2 and Φ, irrespective on the considered wave number.

The same comparison between macro- and micromechanical results has been repeated for the case with softer inclusion. i.e. $\eta_E = 3/50$, $\eta_\nu = 1$. The related plots are reported in Figure 11. Also in this case, numerical micromechanical solutions provide a good agreement with macroscopic analytical results for both U_2/L_1, (Figure 11(a)) and Φ (Figure 11(b)), considering the two wave numbers n=1, n=2.

Finally, in Figure 12 the comparison between the macroscopic analytical solution U_2/L_1 (solid lines), and the micromechanical solution u_2/L_1 (dotted lines) is shown, considering a section line along $\mathbf{e}_1$ that intersects the centroid of the periodic cells, with x_2/L_1=0 as x_1/L_1 varies, see Figure 9. Red and blue curves refer to wave numbers n=1, n=2, respectively. In particular, Figure 12(a) refers to the case with stiffer inclusion, while Figure 12(b) to the case with softer inclusion. In both cases, either for n=1 or n=2, it emerges that the macroscopic analytical solution is able to well reproduce the micromechanical behavior of the actual heterogeneous material. As expected, in the case with stiffer inclusions, more

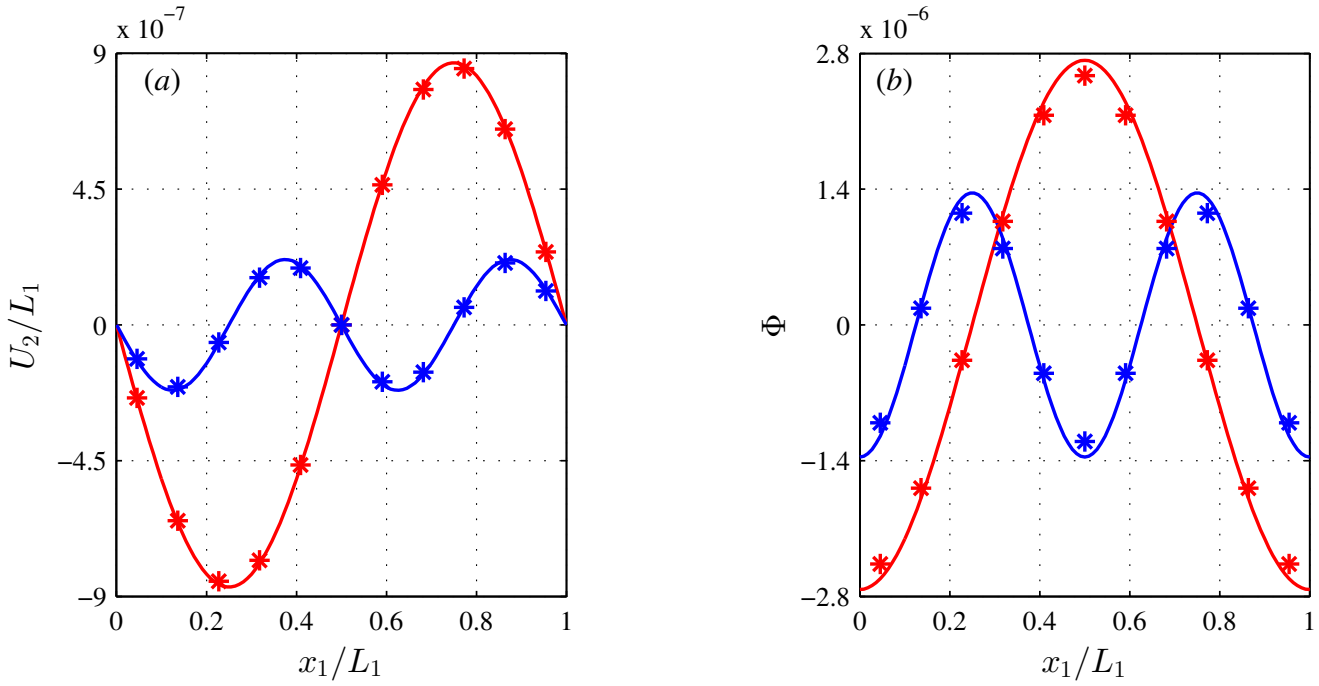

Figure 11: Case with softer inclusion, $\eta_E = 3/50$, η_ν=1. Comparison between macroscopic analytical solutions (solid lines) and macroscopic fields obtained from micro-mechanical results via upscaling relations (stars). Red and blue solid lines and stars refer to harmonic body forces characterized by wave numbers n=1, n=2, respectively. (a) U_2/L_1 vs x_1/L_1; (b) Φ vs x_1/L_1.

pronounced fluctuations around the macroscopic solution are observed in the micromechanical solution, corresponding to the jump between phases.

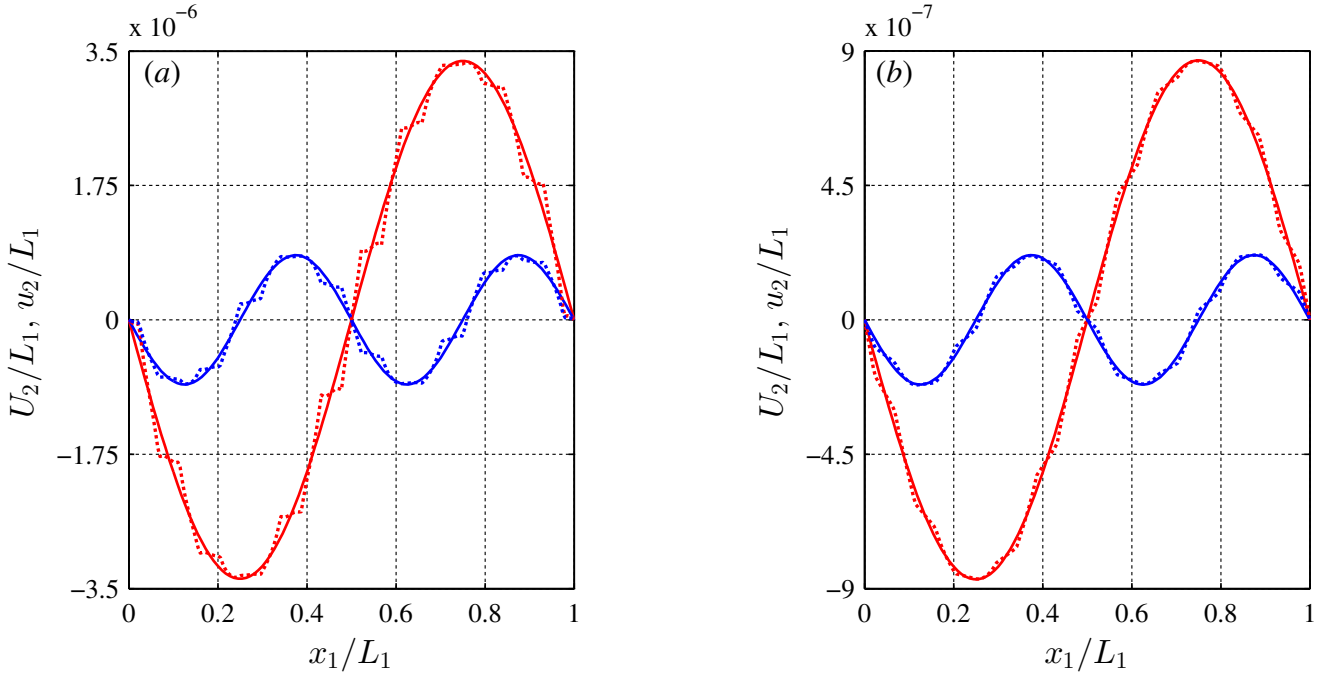

Figure 12: Comparison between dimensionless macroscopic analytical solution U_2/L_1, solid lines, and micromechanical solution u_2/L_1, dotted lines, as x_1/L_1 varies, for x_2/L_1=0. Red and blue curves refer to wave numbers n=1, n=2, respectively. (a) Case with stiffer inclusion; (b) Case with softer inclusion.

4.3. Benchmark 2: Infinite strip undergoing discontinuous periodic forces

As a second benchmark example, we consider an infinite strip of two-phase periodic medium, realized by assembling, along horizontal and vertical directions, the same periodic cells with square inclusions already considered in Section 4.1, see Figure 13. The specimen, of height $\beta\varepsilon$, undergoes a system of discontinuous periodic forces with period $L_1=(4\alpha+\beta)\varepsilon$ and located on both top and bottom sides of the strip, with $\alpha = 4$ and $\beta = 10$. Plane strain conditions are assumed. The same materials considered in

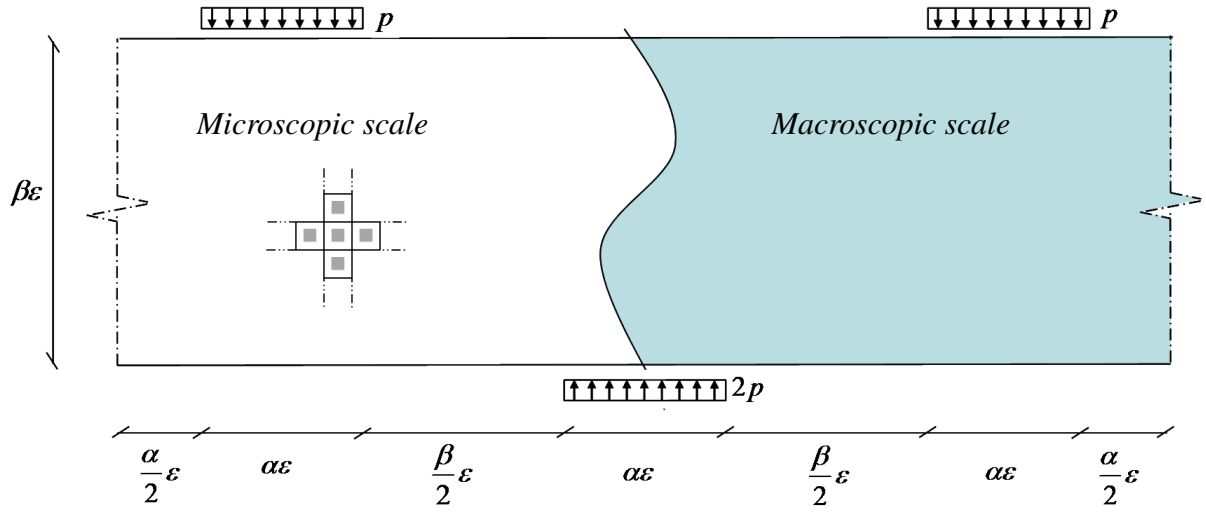

Figure 13: Strip undergoing discontinuous periodic forces: schematic of the heterogeneous medium versus the respective homogenized one (in light blue).

Subsection 4.2 are here taken into account. For both heterogeneous materials, the numerical results of the micro-mechanical model, in terms of displacement and stress components, along a horizontal line located at a distance 9/2 ε from the top side of the strip, are compared with the respective ones obtained considering the micropolar homogenized model.

First the case with stiffer inclusions is considered. In Figure 14(a) the dimensionless micro-mechanical displacement component u_1/L_1 (blue dotted line), and the respective macro-mechanical one U_1/L_1 (red solid line) are plotted versus the dimensionless coordinate x_1/L_1. Analogously, in Figure 14(b) the dimensionless components u_2/L_1 and U_2/L_1 are reported with the same line styles. For both microscopic and macroscopic displacement components a very good agreement is shown. In Figure 15 the macroscopic dimensionless stress components Σ_{11}/E_1, Σ_{22}/E_1, and $\Sigma_{(12)}/E_1$, are compared against the respective microscopic one, i.e. σ_{11}/E_1, σ_{22}/E_1, and $\sigma_{(12)}/E_1$, versus x_1/L_1. The micropolar macroscopic model is able to provide results close to the average of that evaluated with the micro-mechanical model. It is noted that, as expected, micro-mechanical stress components show more pronounced fluctuations that the ones observed on the primal variables u_1 and u_2 in Figure 14.

Secondly, the case with softer inclusions is taken into account. In Figure 16(a), 16(b) the dimensionless micro-mechanical displacement components u_1/L_1, u_2/L_1 (blue dotted lines), and the respective macro-mechanical ones U_1/L_1, U_2/L_1 (red solid lines) are plotted versus x_1/L_1, respectively. Also in this benchmark example, in the case with stiffer inclusions, the fluctuations in the microscopic displacement solution are more evident than in the case with softer inclusions. Moreover, in Figure 17, the macroscopic dimensionless stress components Σ_{11}/E_1, Σ_{22}/E_1, and $\Sigma_{(12)}/E_1$, are compared against the respective microscopic one, i.e. σ_{11}/E_1, σ_{22}/E_1, and σ_{12}/E_1, versus the dimensionless coordinate x_1/L_1. Also in this case of stiffer inclusions, the homogenized solution is in good agreement with the respective micro-mechanical one.

5. Final Remarks

A new micropolar modeling for periodic Cauchy materials based on an asymptotic homogenization scheme has been proposed. The microscopic displacement field is, first, represented via an asymptotic

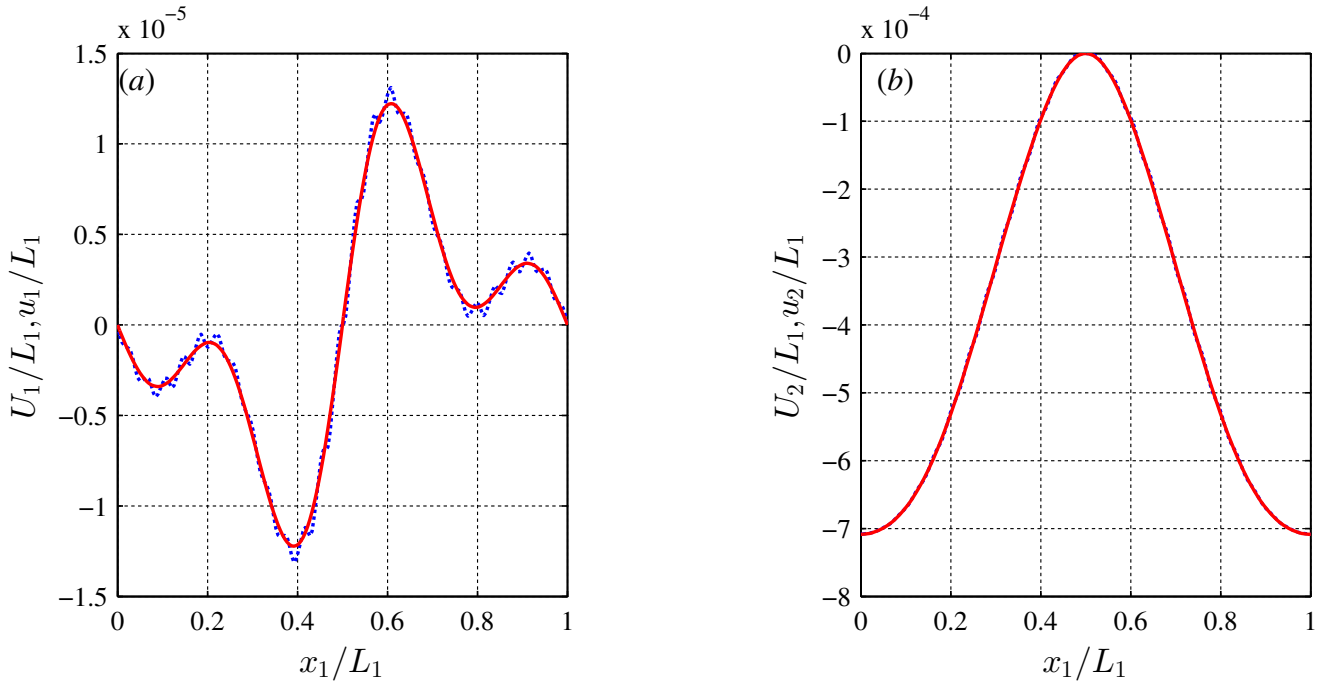

Figure 14: Case with stiffer inclusion. Comparison between dimensionless micro-mechanical displacement components, in blue dotted lines, and the respective macro-mechanical ones, in red solid lines, versus x_1/L_1.(a) Components u_1/L_1, U_1/L_1; (b) components u_2/L_1, U_2/L_1.

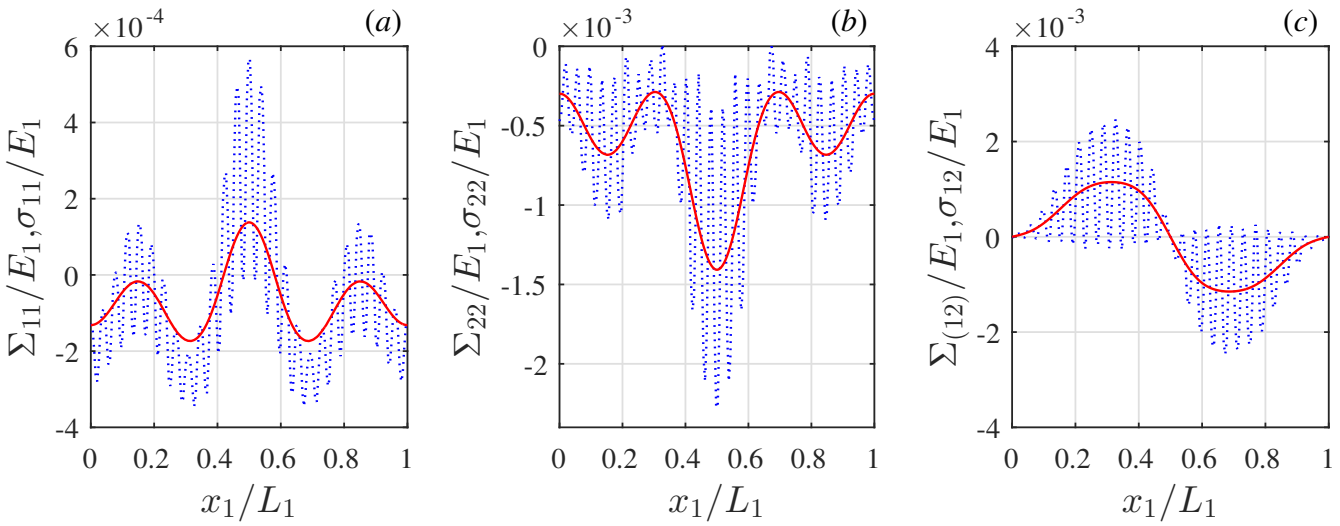

Figure 15: Case with stiffer inclusion. Comparison between dimensionless micro-mechanical stress components, in blue dotted lines, and the respective macro-mechanical ones, in red solid lines, versus x_1/L_1.(a) Components Σ_{11}/E_1, σ_{11}/E_1; (b) components Σ_{22}/E_1, σ_{22}/E_1; (c) components $\Sigma_{(12)}/E_1$, σ_{12}/E_1.

expansion in terms of a micro-structural length. A set of hierarchical cell problems is, thus, obtained, by plugging the asymptotic expansion into the governing equations at the microscopic scale. The solution of such differential problems is given by the perturbation functions that characterize the properties of the microstructure. These perturbation functions are sufficiently regular and locally periodic, i.e. with wave length equal to the size of the periodic cell, and, therefore, they are not dependent on the choice of the reference periodic cell.

The key idea is to propose consistent upscaling relations able to define the macroscopic descriptors (generalized macro-displacement components) of the micropolar continuum in terms of the micro-displacement components, and the perturbation functions. In particular, the micropolar rotation field is obtained by solving a least square minimization procedure that minimizes the difference between the micro infinites-

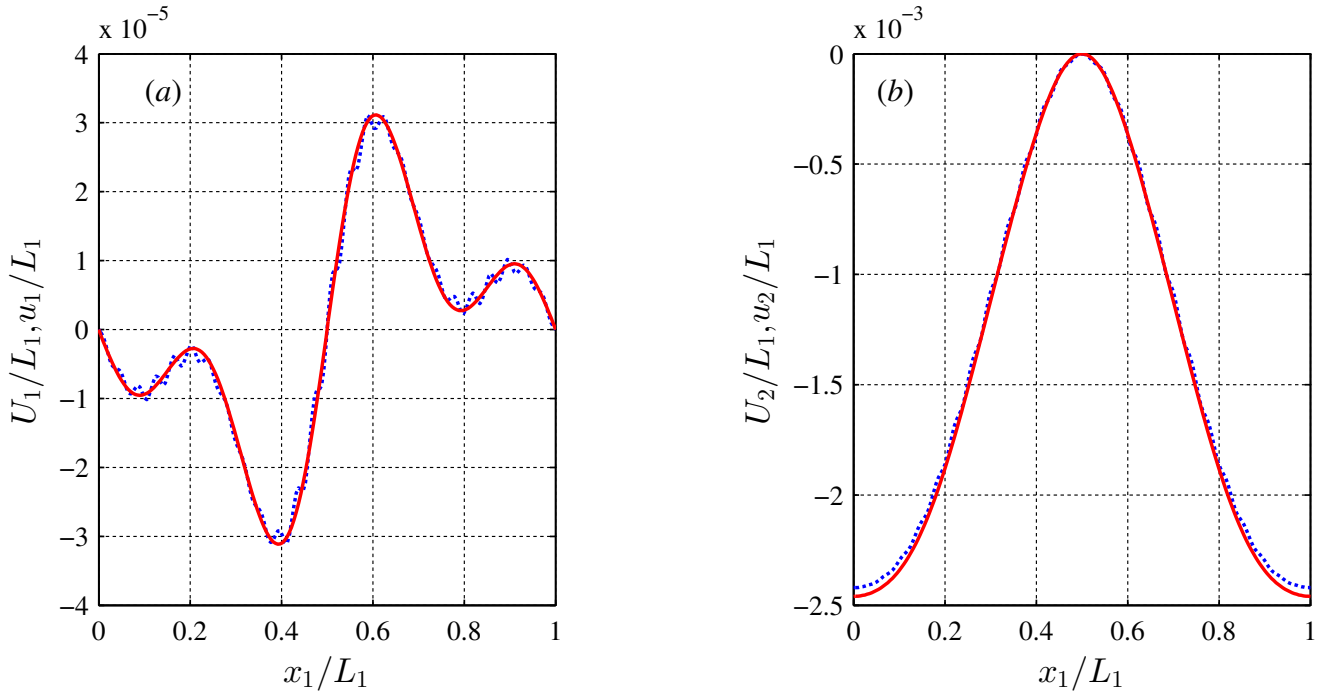

Figure 16: Case with softer inclusion. Comparison between dimensionless micro-mechanical displacement components, in blue dotted lines, and the respective macro-mechanical ones, in red solid lines, versus x_1/L_1.(a) Components u_1/L_1, U_1/L_1; (b) components u_2/L_1, U_2/L_1.

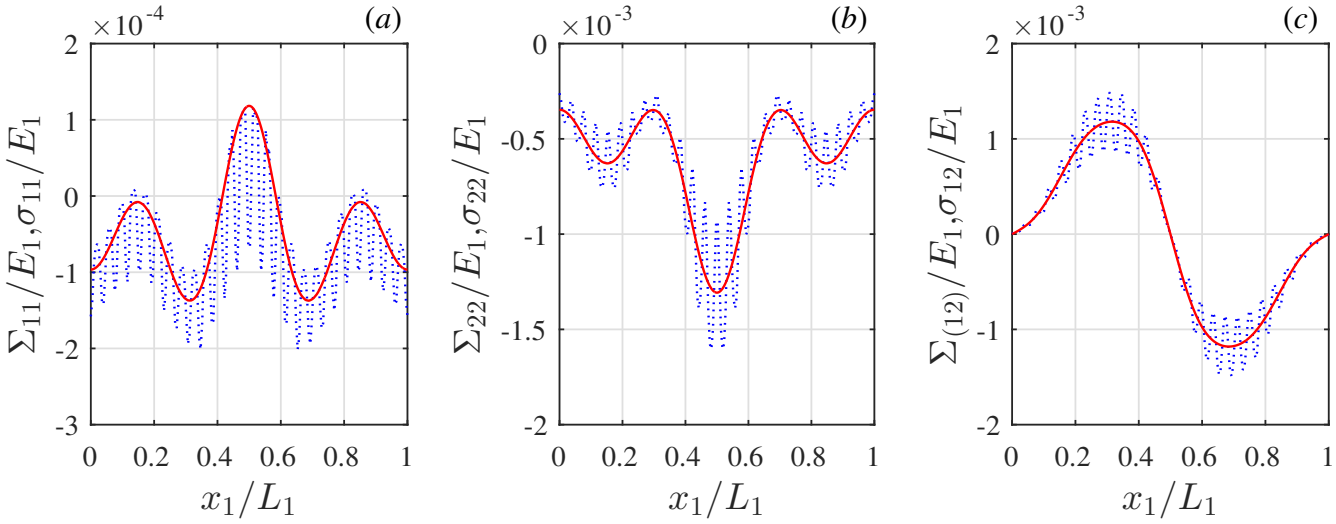

Figure 17: Case with softer inclusion. Comparison between dimensionless micro-mechanical stress components, in blue dotted lines, and the respective macro-mechanical ones, in red solid lines, versus x_1/L_1.(a) Components Σ_{11}/E_1, σ_{11}/E_1; (b) components Σ_{22}/E_1, σ_{22}/E_1; (c) components $\Sigma_{(12)}/E_1$, σ_{12}/E_1.

imal rotation tensor and a properly defined skew-symmetric tensor, depending on the components of both the micropolar rotation tensor and gradients of the perturbation functions. The upscaling relations, linking the actual microscopic displacement field to the generalized macro-displacements, are then specialized to the case where the micro displacement is approximated by an asymptotic expansion truncated at the third order. As concerns the macro-displacements, involved in the asymptotic expansion, a third-order Taylor polynomial is chosen as a function of both macro-displacement components, and displacement gradients components evaluated at a macroscopic reference point. In the third order polynomial only a restricted number of terms, related to the micropolar deformation modes, is retained. To this aim a set of hypotheses, including the satisfaction of the macroscopic governing equations of a first order homogenized

continuum in the absence of body forces, is imposed. Then the kinematic map is consistently derived. By exploiting the kinematic map, the generalized micropolar displacements, the curvature tensor and the micropolar strain tensor are determined.
The overall micropolar elastic properties are derived by exploiting a generalized macro-homogeneity condition, establishing an energy equivalence between the macroscopic and the microscopic scales. It is pointed out that the resulting overall elastic tensors are not affected by the choice of the periodic cell. Moreover, in the limit case of locally homogeneous material, i.e. when the microstructure vanishes, the characteristic lengths tend to zero, thus confirming the absence of non-local effects at the macroscopic scale. The main reasons of this relevant outcome are related, on the one hand, to the proper choice of the upscaling relations and, on the other hand, to the choice of the microscopic average strain energy, involving regular and periodic perturbation functions that consistently describe the material microstructure, and that are obtained solving hierarchical cell problems in the framework of asymptotic techniques. These circumstances represent an improvement in the study of homogenization techniques of periodic Cauchy materials into micromorphic or micropolar equivalent continua.
The capabilities of the proposed homogenization technique in predicting the behavior of periodic materials are assessed through some illustrative examples. Considering a two-phase microstructure characterized by cubic symmetry, first the perturbation functions are derived, by numerically solving cell problems. The related constitutive tensors are, thus, evaluated performing a parametric analysis, as the microstructural mechanical properties vary. Such analysis confirm the model consistency in the case of homogeneous materials. Two benchmark examples, involving periodic forces, are, then, investigated. The macroscopic fields, derived both through analytic and numerical approaches, are compared with those obtained via upscaling relations of the micromechanical solutions. Moreover, the macroscopic fields are qualitatively and quantitatively compared against the respective ones at the microscopic scale.

Acknowledgement

The authors gratefully acknowledge financial support from National Group of Mathematical Physics (GNFM-INdAM), from the Compagnia San Paolo, project MINIERA no. I34I20000380007, from University of Trento, project UNMASKED 2020, project Search for Excellence Ud'A 2019 and project PRIN 2017 - 20173C478N - XFAST-SIMS: Extra fast and accurate simulation of complex structural systems.

Appendix A. Functions occurring in the microdisplacement field $u_1(\mathbf{x},\boldsymbol{\xi})$, $u_2(\mathbf{x},\boldsymbol{\xi})$, and the macroscopic descriptors Φ^0, K_1^0 and K_2^0 in terms of the coefficients $\bar{E}_{11}$, $\bar{E}_{22}$, $\bar{E}_{12}$, $\bar{\kappa}_{122}$, $\bar{\kappa}_{211}$, $\bar{\kappa}_{1222}$

The functions $\mathcal{B}_1^i(\mathbf{x},\boldsymbol{\xi})$ occurring in the polynomial approximation of the microscopic displacement field, equation (37), take the following form depending on the components of the overall elastic tensor of the first order homogeneous continuum and the perturbation functions, i.e.

$$\mathcal{B}_1^1 = x_1 + \varepsilon N_{111}^{(1)}, \tag{A.1}$$

$$\mathcal{B}_1^2 = \varepsilon N_{122}^{(1)}, \tag{A.2}$$

$$\mathcal{B}_1^3 = x_2 + \varepsilon \left(N_{121}^{(1)} + N_{112}^{(1)}\right), \tag{A.3}$$

$$\mathcal{B}_1^4 = \frac{{x_2}^2}{2} + \varepsilon \left(N_{112}^{(1)} x_2 - \frac{N_{121}^{(1)} C_{1212} x_2}{C_{1122}+C_{1212}} - \frac{N_{122}^{(1)} C_{1212}\, x_1}{C_{1122}+C_{1212}}\right) + \varepsilon^2 \left(N_{1122}^{(2)} - \frac{2N_{1212}^{(2)} C_{1212}}{C_{1122}+C_{1212}}\right), \tag{A.4}$$

$$\begin{aligned}\mathcal{B}_1^5 = &-\frac{C_{1212}\, x_2 x_1}{C_{1122}+C_{1212}} + \varepsilon \frac{\left(\left(N_{121}^{(1)} - N_{112}^{(1)}\right) x_1 - N_{111}^{(1)} x_2\right) C_{1212} + N_{121}^{(1)} C_{1122} x_1}{C_{1122}+C_{1212}} + \\ &+ \varepsilon^2 \frac{\left(N_{1211}^{(2)} - 2\,N_{1121}^{(2)}\right) C_{1212} + N_{1211}^{(2)} C_{1122}}{C_{1122}+C_{1212}},\end{aligned} \tag{A.5}$$

$$\mathcal{B}_1^6 = \mathcal{B}_1^{6\text{-}0} + \varepsilon \mathcal{B}_1^{6\text{-}1} + \varepsilon^2 \mathcal{B}_1^{6\text{-}2} + \varepsilon^3 \mathcal{B}_1^{6\text{-}3}, \tag{A.6}$$

where the functions $\mathcal{B}_1^{6\text{-}0}(\mathbf{x})$, $\mathcal{B}_1^{6\text{-}1}(\mathbf{x},\boldsymbol{\xi})$, $\mathcal{B}_1^{6\text{-}2}(\mathbf{x},\boldsymbol{\xi})$ and $\mathcal{B}_1^{6\text{-}3}(\mathbf{x},\boldsymbol{\xi})$ are

$$\mathcal{B}_1^{6\text{-}0} = \frac{{x_2}^3}{6} - \frac{\varsigma_1}{2}\left({C_{1212}}^2 + (C_{1122}+C_{2222})\, C_{1212}\right) x_2 {x_1}^2, \tag{A.7}$$

$$\begin{aligned}\mathcal{B}_1^{6\text{-}1} = &\frac{\varsigma_1}{2}\left(N_{121}^{(1)} C_{1111} C_{1212} + \left(N_{121}^{(1)} - 2N_{112}^{(1)}\right) C_{1122} C_{1212} + \right. \\ &+ \left(N_{121}^{(1)} - N_{112}^{(1)}\right) {C_{1212}}^2 + N_{112}^{(1)}\left(C_{1111}C_{2222} - {C_{1122}}^2\right)\Big) {x_1}^2 + \\ &+ \varsigma_1 \left(\left(N_{122}^{(1)} - N_{111}^{(1)}\right)\left({C_{1212}}^2 + C_{1122}C_{1212}\right) + \left(N_{122}^{(1)} C_{1111} - N_{111}^{(1)} C_{2222}\right) C_{1212}\right) x_1 x_2 + \\ &+ \frac{\varsigma_1}{2}\left(N_{112}^{(1)} C_{2222} C_{1212} + \left(2N_{121}^{(1)} - N_{112}^{(1)}\right) C_{1122} C_{1212} + \right. \\ &+ \left(N_{121}^{(1)} - N_{112}^{(1)}\right) {C_{1212}}^2 + N_{121}^{(1)}\left(C_{1111}C_{2222} - {C_{1122}}^2\right)\Big) {x_2}^2,\end{aligned} \tag{A.8}$$

$$\begin{aligned}\mathcal{B}_1^{6\text{-}2} = &\varsigma_1 \left(\left(2N_{1212}^{(2)} - N_{1111}^{(2)} - N_{1122}^{(2)}\right) {C_{1212}}^2 + N_{1122}^{(2)}\left(C_{1111}C_{2222} - {C_{1122}}^2\right) + \right. \\ &+ \left(2N_{1212}^{(2)} - N_{1111}^{(2)} - 2N_{1122}^{(2)}\right) C_{1122} C_{1212} + \left(N_{1212}^{(2)} C_{1111} - N_{1111}^{(2)} C_{2222}\right) C_{1212}\Big) x_2 + \\ &+ \varsigma_1 \left(\left(N_{1211}^{(2)} + N_{1122}^{(2)} - 2N_{1121}^{(2)}\right) {C_{1212}}^2 - N_{1211}^{(2)}\left(C_{1111}C_{2222} - {C_{1122}}^2\right) + \right. \\ &+ \left(2N_{1211}^{(2)} - N_{1222}^{(2)} - 2N_{1121}^{(2)}\right) C_{1122} C_{1212} + \left(N_{1222}^{(2)} C_{1111} - 2N_{1121}^{(2)} C_{2222}\right) C_{1212}\Big) x_1,\end{aligned} \tag{A.9}$$

$$\begin{aligned}B_1^{6\text{-}3} = &\varsigma_2 \left(\left(N_{12111}^{(3)} + 3N_{12122}^{(3)} - 3N_{11211}^{(3)} - N_{11222}^{(3)}\right) {C_{1212}}^2 + \right. \\ &+ \left(N_{11222}^{(3)} - N_{12111}^{(3)}\right)\left(C_{1111}C_{2222} - {C_{1122}}^2\right) + \\ &+ \left.\left(2N_{12111}^{(3)} + 3N_{12122}^{(3)} - 3N_{11211}^{(3)} - 2N_{11222}^{(3)}\right) C_{1122} + 3\left(N_{12122}^{(3)} C_{1111} - N_{11211}^{(3)} C_{2222}\right)\right) C_{1212},\end{aligned} \tag{A.10}$$

where the parameters ς_1 and ς_2 are

$$\varsigma_1 = \left(C_{1111}C_{2222} - {C_{1122}}^2 - 2C_{1122}C_{1212} - 2{C_{1212}}^2\right)^{-1}, \tag{A.11}$$

$$\varsigma_2 = \left(C_{1111}C_{2222} - 2C_{1122}C_{1212} - 2{C_{1212}}^2\right)^{-1}. \tag{A.12}$$

Analogously, the functions $\mathcal{B}_2^i(\mathbf{x},\boldsymbol{\xi})$ of the equation (37), are

$$\mathcal{B}_2^1 = \varepsilon N_{211}^{(1)}, \tag{A.13}$$

$$\mathcal{B}_2^2 = x_2 + \varepsilon N_{222}^{(1)}, \tag{A.14}$$

$$\mathcal{B}_2^3 = x_1 + \varepsilon \left(N_{221}^{(1)} + N_{212}^{(1)}\right), \tag{A.15}$$

$$\begin{aligned}\mathcal{B}_2^4 = &-\frac{C_{1212}x_2x_1}{C_{1122}+C_{1212}} + \varepsilon\frac{\left(\left(N_{212}^{(1)} - N_{221}^{(1)}\right)x_2 - N_{222}^{(1)}x_1\right)C_{1212} + N_{121}^{(1)}C_{1122}x_1}{C_{1122}+C_{1212}} + \\ &+ \varepsilon^2\frac{\left(N_{1211}^2 - 2N_{1121}^{(2)}\right)C_{1212} + N_{1211}^{(2)}C_{1122}}{C_{1122}+C_{1212}},\end{aligned} \tag{A.16}$$

$$\mathcal{B}_2^5 = \frac{{x_1}^2}{2} + \varepsilon\left(N_{221}^{(1)}x_1 - \frac{N_{212}^{(1)}C_{1212}x_1}{C_{1122}+C_{1212}} - \frac{N_{211}^{(1)}C_{1212}x_2}{C_{1122}+C_{1212}}\right) + \varepsilon^2\left(N_{2211}^{(2)} - \frac{2C_{1212}N_{2121}^{(2)}}{C_{1122}+C_{1212}}\right), \tag{A.17}$$

$$\mathcal{B}_2^6 = \mathcal{B}_2^{6\text{-}0} + \varepsilon\mathcal{B}_2^{6\text{-}1} + \varepsilon^2\mathcal{B}_2^{6\text{-}2} + \varepsilon^3\mathcal{B}_2^{6\text{-}3}, \tag{A.18}$$

where the functions $\mathcal{B}_2^{6\text{-}0}(\mathbf{x})$, $\mathcal{B}_2^{6\text{-}1}(\mathbf{x},\boldsymbol{\xi})$, $\mathcal{B}_2^{6\text{-}2}(\mathbf{x},\boldsymbol{\xi})$ and $\mathcal{B}_2^{6\text{-}3}(\mathbf{x},\boldsymbol{\xi})$ result

$$B_2^{6\text{-}0} = -\frac{{x_1}^3}{6} + \frac{\varsigma_1}{2}\left({C_{1212}}^2 + \left(C_{1122}+C_{1111}\right)C_{1212}\right)x_1{x_2}^2, \tag{A.19}$$

$$\begin{aligned}B_2^{6\text{-}1} = &\frac{\varsigma_1}{2}\left(\left(2N_{221}^{(1)} - N_{212}^{(1)}\right)C_{1122}C_{1212} - N_{212}^{(1)}C_{2222}C_{1212} + \right. \\ &+ \left(N_{221}^{(1)} - N_{212}^{(1)}\right){C_{1212}}^2 - N_{221}^{(1)}\left(C_{1111}C_{2222} - {C_{1122}}^2\right)\Big){x_2}^2 + \\ &+ \varsigma_1\left(\left(N_{222}^{(1)} - N_{211}^{(1)}\right)\left({C_{1212}}^2 + C_{1122}C_{1212}\right) + \left(N_{222}^{(1)}C_{1111} - N_{211}^{(1)}C_{2222}\right)C_{1212}\right)x_1x_2 + \\ &+ \frac{\varsigma_1}{2}\left(N_{221}^{(1)}C_{1111}C_{1212} + \left(N_{221}^{(1)} - 2N_{212}^{(1)}\right)C_{1122}C_{1212} + \right. \\ &+ \left.\left(N_{212}^{(1)} - N_{221}^{(1)}\right){C_{1212}}^2 + N_{212}^{(1)}\left(C_{1111}C_{2222} - {C_{1122}}^2\right)\right){x_1}^2,\end{aligned} \tag{A.20}$$

$$\begin{aligned}B_2^{6\text{-}2} = &\varsigma_1\left(\left(N_{2222}^{(2)} + N_{2211}^{(2)} - 2N_{2121}^{(2)}\right){C_{1212}}^2 - N_{2211}^{(2)}\left(C_{1111}C_{2222} - {C_{1122}}^2\right) + \right. \\ &+ \left.\left(2N_{2211}^{(2)} + N_{2222}^{(2)} - 2N_{2121}^{(2)}\right)C_{1122}C_{1212} + \left(N_{2222}^{(2)}C_{1111} - 2N_{2121}^{(2)}C_{2222}\right)C_{1212}\right)x_1 + \\ &+ \varsigma_1\left(\left(2N_{2212}^{(2)} - N_{2122}^{(2)} - N_{2111}^{(2)}\right){C_{1212}}^2 + N_{2122}^{(2)}\left(C_{1111}C_{2222} - {C_{1122}}^2\right) + \right. \\ &+ \left.\left(2N_{2212}^{(2)} - N_{2111}^{(2)} - 2N_{2111}^{(2)}\right)C_{1122}C_{1212} + \left(2N_{2212}^{(2)}C_{1111} - N_{2111}^{(2)}C_{2222}\right)C_{1212}\right)x_2,\end{aligned} \tag{A.21}$$

$$\begin{aligned}B_2^{6\text{-}3} = &\varsigma_2\left(\left(N_{22111}^{(3)} + 3N_{22122}^{(3)} - 3N_{21211}^{(3)} - N_{21222}^{(3)}\right){C_{1212}}^2 + \right. \\ &+ \left(N_{21222}^{(3)} - N_{22111}^{(3)}\right)\left(C_{1111}C_{2222} - {C_{1122}}^2\right) + \\ &+ \left.\left(2N_{22122}^{(3)} + 3N_{22122}^{(3)} - 3N_{21211}^{(3)} - 2N_{21222}^{(3)}\right)C_{1122} + 3\left(N_{22122}^{(3)}C_{1111} - N_{21211}^{(3)}C_{2222}\right)\right)C_{1212}.\end{aligned} \tag{A.22}$$

The functions $C^i(\boldsymbol{\xi})$ and $\Delta(\boldsymbol{\xi})$ occurring in equation (39) are

$$C^1 = \upsilon\left(N_{111,2}^{(1)} - N_{211,1}^{(1)}\right), \tag{A.23}$$

$$C^2 = \upsilon\left(N_{122,2}^{(1)} - N_{222,1}^{(1)}\right), \tag{A.24}$$

$$C^3 = -\upsilon\left(N_{221,1}^{(1)} - N_{121,2}^{(1)} + N_{212,1}^{(1)} - N_{112,2}^{(1)}\right), \tag{A.25}$$

$$C^4 = \varepsilon\upsilon\left(N_{1122,2}^{(2)} - N_{2122,1}^{(2)} + \frac{\left(2N_{2212,1}^{(2)} - 2N_{1212,2}^{(2)} + N_{112}^{(1)} - N_{121}^{(1)} + N_{222}^{(1)}\right)C_{1212} + N_{221}^{(1)}C_{1122}}{C_{1122}+C_{1212}}\right), \tag{A.26}$$

$$C^5 = \varepsilon\upsilon\left(N^{(2)}_{1211,2} - N^{(2)}_{2211,1} + \frac{\left(2N^{(2)}_{1112,2} - 2N^{(2)}_{2121,1} + N^{(1)}_{111} - N^{(1)}_{212} + N^{(1)}_{221}\right)C_{1212} + N^{(1)}_{221}C_{1122}}{C_{1122} + C_{1212}}\right), \tag{A.27}$$

$$\begin{aligned} C^6 = {} & \varepsilon^2\upsilon\left(N^{(3)}_{11222,2} - N^{(3)}_{12111,2} - N^{(3)}_{21222,1} + N^{(3)}_{22111,1} + \right. \\ & + 3\varsigma_1\left(N^{(3)}_{11222,2} - N^{(3)}_{12111,2} - N^{(3)}_{21222,1} + N^{(3)}_{22111,1}\right)C_{1212}\left(C_{1111} + C_{1122} + C_{1212}\right) + \\ & + \varsigma_1\left(2N^{(2)}_{1212} - N^{(2)}_{1111} - 2N^{(2)}_{1122} + 2N^{(2)}_{2121} - 2N^{(2)}_{2211} - N^{(2)}_{2222}\right)\left({C_{1212}}^2 + C_{1122}C_{1212}\right) + \\ & + \varsigma_1\left(2N^{(2)}_{1212} - N^{(2)}_{2222}\right)C_{1111}C_{1212} - \varsigma_1\left(N^{(2)}_{1111} - 2N^{(2)}_{2121}\right)C_{2222}C_{1212} + \\ & \left. + \varsigma_1\left(2N^{(2)}_{1122} - N^{(2)}_{2211}\right)\left(C_{1111}C_{2222} - {C_{1122}}^2\right)\right), \end{aligned} \tag{A.28}$$

where the υ parameter takes the following form

$$\upsilon = \left(N^{(1)}_{122,1} + N^{(1)}_{211,2} - N^{(1)}_{212,1} - N^{(1)}_{121,2} - 2\right). \tag{A.29}$$

The functions $\mathcal{D}^i(\boldsymbol{\xi})$ and $\mathcal{G}^i(\boldsymbol{\xi})$ in equations (40) are

$$D^1 = \frac{\upsilon\left(N^{(1)}_{222,1} - N^{(1)}_{122,2}\right)C_{1212}}{C_{1122} + C_{1212}}, \tag{A.30}$$

$$D^2 = \upsilon\left(N^{(1)}_{121,2} - N^{(1)}_{221,1}\right) + \upsilon\frac{\left(N^{(1)}_{212,1} - N^{(1)}_{112,2} - 2\right)C_{1212} - C_{1122}}{C_{1122} + C_{1212}}, \tag{A.31}$$

$$\begin{aligned} D^3 = {} & \varepsilon\upsilon\varsigma_1\left(2\left(N^{(2)}_{2121,1} - N^{(2)}_{1121,2} - 2N^{(2)}_{2222,1} + 2N^{(3)}_{1222,2}\right)\left(C_{2222} + C_{1122} + C_{1212}\right) + \right. \\ & + \left(N^{(1)}_{122} + N^{(1)}_{212} - N^{(1)}_{111} - N^{(1)}_{221}\right)\left({C_{1212}}^2 + C_{1122}C_{1212}\right) + \\ & + \left(N^{(1)}_{212} - N^{(1)}_{111}\right)C_{2222}C_{1212} + N^{(1)}_{122}C_{1111}C_{1212} + \\ & \left. + N^{(1)}_{221}\left(C_{1111}C_{2222} - {C_{1122}}^2\right)\right) + \varepsilon\upsilon\left(N^{(2)}_{2211,1} - N^{(2)}_{1211,2}\right), \end{aligned} \tag{A.32}$$

$$G^1 = \upsilon\left(N^{(1)}_{112,2} - N^{(1)}_{212,1}\right) - \upsilon\frac{\left(N^{(1)}_{121,2} - N^{(1)}_{221,1} - 2\right)C_{1212} + C_{1122}}{C_{1122} + C_{1212}}, \tag{A.33}$$

$$G^2 = \frac{\upsilon\left(N^{(1)}_{211,1} - N^{(1)}_{111,2}\right)C_{1212}}{C_{1122} + C_{1212}}, \tag{A.34}$$

$$\begin{aligned} G^3 = {} & \varepsilon\upsilon\varsigma_1\left(2\left(N^{(2)}_{1212,2} - N^{(2)}_{2212,1} - 2N^{(2)}_{1111,2} + 2N^{(3)}_{2111,1}\right)\left(C_{1111} + C_{1122} + C_{1212}\right) + \right. \\ & + \left(N^{(1)}_{211} + N^{(1)}_{121} - N^{(1)}_{222} - N^{(1)}_{112}\right)\left({C_{1212}}^2 + C_{1122}C_{1212}\right) + \\ & + \left(N^{(1)}_{121} - N^{(1)}_{222}\right)C_{1111}C_{1212} + N^{(1)}_{211}C_{2222}C_{1212} + \\ & \left. + N^{(1)}_{112}\left(C_{1111}C_{2222} - {C_{1122}}^2\right)\right) + \varepsilon\upsilon\left(N^{(2)}_{1122,2} - N^{(2)}_{2122,1}\right). \end{aligned} \tag{A.35}$$

Appendix B. Microscopic and macroscopic constitutive equations in equivalent matrix notation

Considering a generic material point at the microscopic level the displacement vector of is defined as $\underline{\mathbf{u}} = \left\{ \begin{array}{cc} u_1 & u_2 \end{array} \right\}^T$ and the constitutive equations, relating the strain vector $\underline{\boldsymbol{\varepsilon}} = \left\{ \begin{array}{ccc} \varepsilon_{11} & \varepsilon_{22} & \sqrt{2}\varepsilon_{12} \end{array} \right\}^T$ and stress vector $\underline{\boldsymbol{\sigma}} = \left\{ \begin{array}{ccc} \sigma_{11} & \sigma_{22} & \sqrt{2}\sigma_{12} \end{array} \right\}^T$, are

$$\underline{\boldsymbol{\sigma}} = \underline{\underline{\mathbf{C}}}^m\underline{\boldsymbol{\varepsilon}}, \tag{B.1}$$

where $\underline{\underline{\mathbf{C}}}^m$ is the microscopic elastic matrix. The Equation (B.1) in component form specializes in

$$\left\{ \begin{array}{c} \sigma_{11} \\ \sigma_{22} \\ \sqrt{2}\sigma_{12} \end{array} \right\} = \left[\begin{array}{ccc} C^m_{1111} & C^m_{1122} & \sqrt{2}C^m_{1112} \\ C^m_{1122} & C^m_{2222} & \sqrt{2}C^m_{2212} \\ \sqrt{2}C^m_{1112} & \sqrt{2}C^m_{2212} & 2C^m_{1212} \end{array} \right] \left\{ \begin{array}{c} \varepsilon_{11} \\ \varepsilon_{22} \\ \sqrt{2}\varepsilon_{12} \end{array} \right\}. \tag{B.2}$$

At the macroscopic level, instead, the generic material point is endowed with independent translational and rotational degrees of freedom collected in the generalized displacement vector $\underline{\mathbf{U}} = \left\{ \begin{array}{ccc} U_1 & U_2 & \Phi \end{array} \right\}^T$. The asymmetric micropolar strain vector and the curvature vector are

$$\begin{aligned} \underline{\boldsymbol{\Gamma}} &= \left\{ \begin{array}{cccc} \Gamma_{11} & \Gamma_{22} & \Gamma_{12} & \Gamma_{21} \end{array} \right\}^T, \\ \underline{\mathbf{K}} &= \left\{ \begin{array}{cc} K_1 & K_2 \end{array} \right\}^T. \end{aligned} \tag{B.3}$$

Moreover, the macroscopic stress vector and the couple stress vector results as

$$\begin{aligned} \underline{\boldsymbol{\Sigma}} &= \left\{ \begin{array}{cccc} \Sigma_{11} & \Sigma_{22} & \Sigma_{12} & \Sigma_{21} \end{array} \right\}^T, \\ \underline{\mathbf{M}} &= \left\{ \begin{array}{cc} M_1 & M_2 \end{array} \right\}^T, \end{aligned} \tag{B.4}$$

Finally, the micropolar constitutive relations at the macroscopic scale read as

$$\left\{ \begin{array}{c} \underline{\boldsymbol{\Sigma}} \\ \underline{\mathbf{M}} \end{array} \right\} = \left[\begin{array}{cc} \underline{\underline{\mathbf{G}}}^M & \underline{\underline{\mathbf{Y}}}^M \\ \underline{\underline{\mathbf{Y}}}^{MT} & \underline{\underline{\mathbf{S}}}^M \end{array} \right] \left\{ \begin{array}{c} \underline{\boldsymbol{\Gamma}} \\ \underline{\mathbf{K}} \end{array} \right\}. \tag{B.5}$$

At this point, the equation (B.3) can be recast in the generalized micropolar strain vector $\underline{\mathbf{E}}^{(mp)} = \left\{ \begin{array}{cc} \underline{\boldsymbol{\Gamma}} & \underline{\mathbf{K}} \end{array} \right\}^T$, analogously, the equation (B.4) can be recast in the generalized stress vector is defined as $\underline{\mathbf{S}}^{(mp)} = \left\{ \begin{array}{cc} \underline{\boldsymbol{\Sigma}} & \underline{\mathbf{M}} \end{array} \right\}^T$. As a consequence, the micropolar constitutive relations take the following form

$$\underline{\mathbf{S}}^{(mp)} = \underline{\underline{\mathbf{C}}}^{M(mp)} \underline{\mathbf{E}}^{(mp)}. \tag{B.6}$$

Equations (B.5) and (B.6) in component form result

$$\left\{ \begin{array}{c} \Sigma_{11} \\ \Sigma_{22} \\ \Sigma_{12} \\ \Sigma_{21} \\ \mathrm{M}_1 \\ \mathrm{M}_2 \end{array} \right\} = \left[\begin{array}{cccccc} G_{1111} & G_{1122} & G_{1112} & G_{1121} & Y_{111} & Y_{211} \\ G_{1122} & G_{2222} & G_{2212} & G_{2221} & Y_{221} & Y_{222} \\ G_{1112} & G_{2212} & G_{1212} & G_{1221} & Y_{121} & Y_{122} \\ G_{1121} & G_{2221} & G_{1221} & G_{2121} & Y_{211} & Y_{212} \\ Y_{111} & Y_{221} & Y_{121} & Y_{211} & \mathrm{S}_{11} & \mathrm{S}_{12} \\ Y_{211} & Y_{222} & Y_{212} & Y_{212} & \mathrm{S}_{12} & \mathrm{S}_{22} \end{array} \right] \left\{ \begin{array}{c} \Gamma_{11} \\ \Gamma_{22} \\ \Gamma_{12} \\ \Gamma_{21} \\ \mathrm{K}_1 \\ \mathrm{K}_2 \end{array} \right\}. \tag{B.7}$$

Finally, by splitting the symmetric and skew-symmetric components of the asymmetric micropolar stress and the micropolar strain, as in equation (62), it results

$$\left\{ \begin{array}{c} \Sigma_{11} \\ \Sigma_{22} \\ \Sigma_{(12)} \\ \Sigma_{[21]} \\ \mathrm{M}_1 \\ \mathrm{M}_2 \end{array} \right\} = \left[\begin{array}{cccccc} G_{1111} & G_{1122} & G_{11(12)} & G_{11[12]} & Y_{111} & Y_{112} \\ G_{1122} & G_{2222} & G_{22(12)} & G_{22[12]} & Y_{221} & Y_{222} \\ G_{11(12)} & G_{22(12)} & G_{(12)(12)} & G_{(12)[12]} & Y_{(12)1} & Y_{(12)2} \\ G_{11[12]} & G_{22[12]} & G_{(12)[12]} & G_{[12][12]} & Y_{[12]1} & Y_{[12]2} \\ Y_{111} & Y_{221} & Y_{(12)1} & Y_{[12]1} & \mathrm{S}_{11} & \mathrm{S}_{12} \\ Y_{112} & Y_{222} & Y_{(12)2} & Y_{[12]2} & \mathrm{S}_{12} & \mathrm{S}_{22} \end{array} \right] \left\{ \begin{array}{c} \Gamma_{11} \\ \Gamma_{22} \\ 2\Gamma_{(12)} \\ 2\Gamma_{[12]} \\ \mathrm{K}_1 \\ \mathrm{K}_2 \end{array} \right\}. \tag{B.8}$$

References

[1] Albert Edward Green and Ronald S Rivlin. Multipolar continuum mechanics. *Archive for Rational Mechanics and Analysis*, 17(2):113–147, 1964.

[2] Raymond David Mindlin. Micro-structure in linear elasticity. *Archive for Rational Mechanics and Analysis*, 16(1): 51–78, 1964.

[3] P. Germain. The method of virtual power in continuum mechanics. part 2: microstructure. *SIAM Journal of Applied Mathematics*, 25:556–575, 1973.

[4] E. Sanchez-Palencia. Comportements local et macroscopique d'un type de milieux physiques heterogenes. *International Journal of Engineering Science*, 12(4):331–351, 1974.

[5] N.S. Bakhvalov and G.P. Panasenko. *Homogenization: Averaging Processes in Periodic Media*. Kluwer Academic Publishers, Dordrecht-Boston-London, 1984.

[6] B. Gambin and E. Kröner. Higher order terms in the homogenized stress-strain relation of periodic elastic media. physica status solidi (b). *International Journal of Engineering Science*, 151(2):513–519, 1989.

[7] SA Meguid and AL Kalamkarov. Asymptotic homogenization of elastic composite materials with a regular structure. *International journal of solids and structures*, 31(3):303–316, 1994.

[8] Jacob Fish and Wen Chen. Higher-order homogenization of initial/boundary-value problem. *Journal of engineering mechanics*, 127(12):1223–1230, 2001.

[9] Igor V Andrianov, Vladimir I Bolshakov, Vladyslav V Danishevs' kyy, and Dieter Weichert. Higher order asymptotic homogenization and wave propagation in periodic composite materials. In *Proceedings of the Royal Society of London A: Mathematical, Physical and Engineering Sciences*, volume 464, pages 1181–1201. The Royal Society, 2008.

[10] Grigory Panasenko. Boundary conditions for the high order homogenized equation: laminated rods, plates and composites. *Comptes Rendus Mecanique*, 337(1):8–14, 2009.

[11] A. Bacigalupo. Second-order homogenization of periodic materials based on asymptotic approximation of the strain energy: formulation and validity limits. *Meccanica*, 49(6):1407–1425, 2014.

[12] E Bosco, RHJ Peerlings, and MGD Geers. Asymptotic homogenization of hygro-thermo-mechanical properties of fibrous networks. *International Journal of Solids and Structures*, 115:180–189, 2017.

[13] Francesca Fantoni, Andrea Bacigalupo, and Marco Paggi. Multi-field asymptotic homogenization of thermo-piezoelectric materials with periodic microstructure. *International Journal of Solids and Structures*, 120:31–56, 2017.

[14] J.R. Willis. Variational and related methods for the overall properties of composites. volume 21 of *Advances in Applied Mechanics*, pages 1 – 78. Elsevier, 1981.

[15] V.P. Smyshlyaev and K.D. Cherednichenko. On rigorous derivation of strain gradient effects in the overall behaviour of periodic heterogeneous media. *Journal of the Mechanics and Physics of Solids*, 48(6):1325–1357, 2000.

[16] R.H.J. Peerlings and N.A. Fleck. Computational evaluation of strain gradient elasticity constants. *International Journal for Multiscale Computational Engineering*, 2(4), 2004.

[17] A. Bacigalupo and L. Gambarotta. Second-gradient homogenized model for wave propagation in heterogeneous periodic media. *International Journal of Solids and Structures*, 51(5):1052–1065, 2014.

[18] D. Bigoni and W. J. Drugan. Analytical derivation of Cosserat moduli via homogenization of heterogeneous elastic materials. *J Appl Mech*, 74:741–753, 2007.

[19] Uwe Mühlich, Lutz Zybell, and Meinhard Kuna. Estimation of material properties for linear elastic strain gradient effective media. *European Journal of Mechanics-A/Solids*, 31(1):117–130, 2012.

[20] M. Bacca, D. Bigoni, F. Dal Corso, and D. Veber. Mindlin second-gradient elastic properties from dilute two-phase cauchy-elastic composites. part i: Closed form expression for the effective higher-order constitutive tensor. *International Journal of Solids and Structures*, 50(24):4010 – 4019, 2013. ISSN 0020-7683.

[21] M. Bacca, D. Bigoni, F. Dal Corso, and D. Veber. Mindlin second-gradient elastic properties from dilute two-phase cauchy-elastic composites part ii: Higher-order constitutive properties and application cases. *International Journal of Solids and Structures*, 50(24):4020 – 4029, 2013. ISSN 0020-7683.

[22] Mattia Bacca, Francesco Dal Corso, Daniele Veber, and Davide Bigoni. Anisotropic effective higher-order response of heterogeneous cauchy elastic materials. *Mechanics Research Communications*, 54:63–71, 2013.

[23] Andrea Bacigalupo, Marco Paggi, F Dal Corso, and D Bigoni. Identification of higher-order continua equivalent to a cauchy elastic composite. *Mechanics Research Communications*, doi.org/10.1016/j.mechrescom.2017.07.002, 2017.

[24] Geralf Hütter. Homogenization of a cauchy continuum towards a micromorphic continuum. *Journal of the Mechanics and Physics of Solids*, 99:394–408, 2017.

[25] Samuel Forest. Mechanics of generalized continua: construction by homogenizaton. *Le Journal de Physique IV*, 8(PR4): Pr4–39, 1998.

[26] O Van der Sluis, PHJ Vosbeek, PJG Schreurs, et al. Homogenization of heterogeneous polymers. *International Journal of Solids and Structures*, 36(21):3193–3214, 1999.

[27] F. Feyel. A multilevel finite element method (fe2) to describe the response of highly non-linear structures using generalized continua. *Comput Method Appl M*, 192:3233–3244, 2003.

[28] V.G. Kouznetsova, M.G.D. Geers, and W.A.M. Brekelmans. Multi-scale second-order computational homogenization

of multi-phase materials: a nested finite element solution strategy. *Computer Methods in Applied Mechanics and Engineering*, 193(48):5525–5550, 2004.

[29] Xi Yuan, Yoshihiro Tomita, and Tomoaki Andou. A micromechanical approach of nonlocal modeling for media with periodic microstructures. *Mechanics Research Communications*, 35(1-2):126–133, 2008.

[30] Łukasz Kaczmarczyk, Chris J Pearce, and Nenad Bićanić. Scale transition and enforcement of rve boundary conditions in second-order computational homogenization. *International Journal for Numerical Methods in Engineering*, 74(3): 506–522, 2008.

[31] Tarek I Zohdi and Peter Wriggers. *An introduction to computational micromechanics*. Springer Science & Business Media, 2008.

[32] A. Bacigalupo and L. Gambarotta. Second-order computational homogenization of heterogeneous materials with periodic microstructure. *ZAMM Journal of Applied Mathematics and Mechanics*, 90:796–811, 2010.

[33] M. L. De Bellis and D. Addessi. A Cosserat based multi–scale model for masonry structures. *International Journal for Multiscale Computational Engineering*, 9(5):543–563, 2011.

[34] S. Forest and D.K. Trinh. Generalized continua and non-homogeneous boundary conditions in homogenisation methods. *ZAMM-Journal of Applied Mathematics and Mechanics/Zeitschrift für Angewandte Mathematik und Mechanik*, 91(2): 90–109, 2011.

[35] Xikui Li, Junbo Zhang, and Xue Zhang. Micro-macro homogenization of gradient-enhanced cosserat media. *European Journal of Mechanics-A/Solids*, 30(3):362–372, 2011.

[36] I Temizer and Peter Wriggers. Homogenization in finite thermoelasticity. *Journal of the Mechanics and Physics of Solids*, 59(2):344–372, 2011.

[37] Tomislav Lesičar, Zdenko Tonković, and Jurica Sorić. C1 continuity finite element formulation in second-order computational homogenization scheme. *Journal of Multiscale Modelling*, 4(04):1250013, 2012.

[38] YJ Chen, F Scarpa, YJ Liu, and JS Leng. Elasticity of anti-tetrachiral anisotropic lattices. *International Journal of Solids and Structures*, 50(6):996–1004, 2013.

[39] F El Halabi, D González, A Chico, and M Doblaré. Fe2 multiscale in linear elasticity based on parametrized microscale models using proper generalized decomposition. *Computer Methods in Applied Mechanics and Engineering*, 257:183–202, 2013.

[40] Tomislav Lesičar, Zdenko Tonković, and Jurica Sorić. A second-order two-scale homogenization procedure using c-1 macrolevel discretization. *Computational mechanics*, 54(2):425–441, 2014.

[41] A Salvadori, E Bosco, and D Grazioli. A computational homogenization approach for li-ion battery cells: Part 1–formulation. *Journal of the Mechanics and Physics of Solids*, 65:114–137, 2014.

[42] D. Addessi, M. L. De Bellis, and E. Sacco. A micromechanical approach for the cosserat modeling of composites. *Meccanica*, 51(3):569–592, 2016.

[43] V. Sepe, F. Auricchio, S. Marfia, and E. Sacco. Homogenization techniques for the analysis of porous sma. *Computational Mechanics*, 57(5):755–772, May 2016.

[44] Raja Biswas and Leong Hien Poh. A micromorphic computational homogenization framework for heterogeneous materials. *Journal of the Mechanics and Physics of Solids*, 102:187–208, 2017.

[45] Maria Laura De Bellis and Andrea Bacigalupo. Auxetic behavior and acoustic properties of microstructured piezoelectric strain sensors. *Smart Materials and Structures*, 26(8):085037, 2017.

[46] Patrizia Trovalusci, Maria Laura De Bellis, and Renato Masiani. A multiscale description of particle composites: From lattice microstructures to micropolar continua. *Composites Part B: Engineering*, 128:164 – 173, 2017. ISSN 1359-8368.

[47] Emanuele Reccia, Maria Laura De Bellis, Patrizia Trovalusci, and Renato Masiani. Sensitivity to material contrast in homogenization of random particle composites as micropolar continua. *Composites Part B: Engineering*, 136:39 – 45, 2018.

[48] Michele Marino, Blaž Hudobivnik, and Peter Wriggers. Computational homogenization of polycrystalline materials with the virtual element method. *Computer Methods in Applied Mechanics and Engineering*, 355:349–372, 2019.

[49] Christoph Böhm, Blaž Hudobivnik, Michele Marino, and Peter Wriggers. Electro-magneto-mechanically response of polycrystalline materials: Computational homogenization via the virtual element method. *Computer Methods in Applied Mechanics and Engineering*, 380:113775, 2021.

[50] D. Addessi, M. L. De Bellis, and E. Sacco. Micromechanical analysis of heterogeneous materials subjected to overall cosserat strains. *Mechanics Research Communications*, 54:27 – 34, 2013.

[51] Maria Laura De Bellis, Andrea Bacigalupo, and Giorgio Zavarise. Characterization of hybrid piezoelectric nanogenerators through asymptotic homogenization. *Computer Methods in Applied Mechanics and Engineering*, 355:1148–1186, 2019.